

UNIVERSITY COLLEGE LONDON

MSCI PHYSICS

PHASM201: PHYSICS PROJECT

---

# Entropy Production In Small Systems

---

*Author:*  
Henry CHARLESWORTH

*Supervisor:*  
Professor Ian FORD

April 1, 2014

## Abstract

The entropy production of a Brownian particle in a non-isothermal and non-stationary heat bath is studied within the context of stochastic thermodynamics. The full phase space dynamics are considered, with a variational approach being employed to obtain an approximate solution in the limit of large damping to the Kramers equation which governs the probability density function of the system. This allows for the calculation of simple expressions for the average rate of entropy production, as well as the average rate of the three constituent components related to the housekeeping and the excess heat. This is then compared with an equivalent description of the system using stochastic differential equations, for which an average as well as a distribution of the entropy production can be obtained by the simulation of many stochastic particle trajectories. Using this method also allows us to check whether the relevant entropy related fluctuation relations hold for this system. The particular case of a sinusoidally varying quadratic temperature profile is looked at in detail, and although there is reasonable agreement between the averages obtained through both approaches there are also clearly some problems which are not resolved and still need to be investigated more closely.

# Contents

<b>1</b>	<b>Introduction</b>	<b>2</b>
<b>2</b>	<b>Stochastic Thermodynamics</b>	<b>4</b>
2.1	Stochastic Master Equations and the Fokker-Planck Equation . . . . .	4
2.2	Stochastic Calculus . . . . .	5
2.3	Stochastic Differential Equations and Relationship with Generalized Fokker-Planck Equations . .	6
2.4	Entropy In Stochastic Thermodynamics . . . . .	6
2.5	Splitting the Entropy into Three Components . . . . .	7
2.6	Fluctuation Relations . . . . .	8
<b>3</b>	<b>Brownian Particle in a Non-Isothermal Heat Bath</b>	<b>10</b>
3.1	Basic Description of System . . . . .	10
3.2	General Expression for Average Entropy Production Rate . . . . .	12
3.3	Calculation of an Approximate PDF . . . . .	13
3.4	Approximate Rate of Entropy Production . . . . .	17
<b>4</b>	<b>Sinusoidally Varying Quadratic Temperature Profile</b>	<b>20</b>
4.1	Stationary Temperature Profile . . . . .	21
4.2	Non-Stationary Temperature Profile . . . . .	23
4.3	Improving the model for $\rho$ . . . . .	34
<b>5</b>	<b>Conclusion</b>	<b>36</b>
<b>A</b>	<b>Code to Simulate Particle Trajectories</b>	<b>37</b>
<b>B</b>	<b>References</b>	<b>45</b>

# Chapter 1

## Introduction

The huge success of equilibrium thermodynamics lies in its ability to provide a description of systems with an enormous number of degrees of freedom in terms of just a few simple state variables. At the heart of this description is entropy, a quantity which the second law of thermodynamics famously states can only ever increase and is used to explain the apparent irreversibility of all non-idealized macroscopic processes. The second law of thermodynamics has a vast collection of empirical evidence backing it up as well as being in agreement with our everyday experience of the one way nature of most processes, but is in many ways difficult to fully understand and as such still attracts a lot of discussion today. In particular, how can there be a physical quantity which only ever increases given that the underlying microscopic laws are entirely time reversible, a problem known as Loschmidt's paradox[1]. The simple answer is that there cannot be, and so the modern interpretation of entropy has been to view it as a measure of information or of our uncertainty in the microscopic details of the system, but even with this interpretation there are questions to address. One potential problem is Liouville's theorem which proves for Hamiltonian systems that the flow in phase space is incompressible, making entropy as defined by Gibbs a constant of motion [2]. However Liouville's theorem only applies to systems which are evolving deterministically according to Hamilton's equations of motion and the fact is that trying to model every component of a complicated system deterministically is a fool's game, and cannot be done in practice. Indeed if this were not the case then there would never have been the need for the subject of thermodynamics in the first place! If we accept that our description must necessarily contain some form of coarse-graining, where generally we will separate the total system into a system of interest and its environment and provide only roughly specified interactions between them then it is clear that our uncertainty about the system's details will naturally increase. Loschmidt's paradox is avoided by realizing that given an initial configuration this would be the case regardless of which direction in time we evolved the system, with the apparent irreversibility of the process arising only as a consequence of the disparity in the effect of the coupling on the system and the environment because of their relative sizes. This report is concerned with entropy specifically as it is defined in the emerging subject of stochastic thermodynamics, which provides a framework for describing small systems that are interacting with an environment, and where generally fluctuations play a dominant role. Here entropy is constructed manifestly as a measure of irreversibility and defined on the level of individual stochastic trajectories in such a way that it remains consistent with the standard thermodynamic definition[3]. As well as having potential applications in a number of different fields[4], the framework allows us to look closely at the nature of the second law of thermodynamics and the physical origins of irreversibility.

The prototypical system of study in stochastic thermodynamics has been a Brownian particle in a heat bath

which is then driven away from equilibrium in some way. Despite being a simple system it allows for the application of all of the key principles in stochastic thermodynamics and as such a number of variants in the type of driving applied to this system have been studied [3, 5, 6]. Additionally under certain circumstances the use of time-dependent laser traps has allowed for quantitative experimental probing of some of the fluctuation relations (introduced in section 2.6), as individual particle trajectories for this kind of system can be traced[6]. The objective of this project was to look at the case of a Brownian particle in a non-isothermal heat bath with a temperature profile which varies both spatially and temporally and to calculate the entropy produced in such a process both analytically and by simulating many particle trajectories. In addition to this the entropy production can be split into three different components[13], each of which has a particular thermodynamic interpretation and so we wanted to calculate each of these and look at their distributions, as well as checking that they and the total entropy obey the relevant fluctuation relations.

# Chapter 2

## Stochastic Thermodynamics

This chapter first gives a brief introduction to some techniques which can be used to model the dynamics of a stochastic system before going on to introduce stochastic thermodynamics and the definition of entropy. The main idea behind stochastic thermodynamics is to model the interaction of a system and its environment with additional stochastic terms in the system's equations of motion, and then to extend various classical thermodynamic quantities such as heat, work done and entropy so that they can be meaningfully defined for individual stochastic trajectories. In the final section some of the entropy related fluctuation theorems are introduced, which under certain conditions make exact thermodynamic statements about non-equilibrium systems[9].

### 2.1 Stochastic Master Equations and the Fokker-Planck Equation

We start by considering a simple stochastic system which can occupy a set of finite states  $\{x_i\}$  at discrete times labelled by  $t_n$  where  $n$  is an integer. Demanding that the system is Markovian, so that the probability of being in the state  $x_m$  at time  $t_{n+1}$  depends only upon the state of the system at time  $t_n$ , (i.e. that it has no memory of its previous history), a master equation governing the evolution of the probability distribution can then be written[7]:

$$p(x_m, t_{n+1}) = \sum_{m'} p(x_m, t_{n+1} | x_{m'}, t_n) p(x_{m'}, t_n) \quad (2.1)$$

This is then be generalized to systems which can occupy a continuous range of states  $x$  by using a probability density  $p(x,t)$  and introducing a transition probability density  $T(\Delta x|x, t)$  which is the probability density of making a transition of  $\Delta x$  in a time  $\tau$  given a value of  $x$  and  $t$ . This gives

$$p(x, t + \tau) = \int p(x - \Delta x, t) T(\Delta x|x - \Delta x, t) d\Delta x \quad (2.2)$$

a result known as the Chapman-Kolmogorov equation[8]. Assuming that  $p(x,t)$  and  $T(\Delta x|x, t)$  are both continuous functions of the variable  $x$  we can take a Taylor expansion of the integrand of equation 2.2 so that:

$$p(x - \Delta x, t) T(\Delta x|x - \Delta x, t) = p(x, t) T(\Delta x|x, t) + \sum_{n=1}^{\infty} \frac{1}{n!} (-\Delta x)^n \frac{\partial^n (p(x, t) T(\Delta x|x, t))}{\partial x^n} \quad (2.3)$$

Then using the fact that normalization requires  $\int T(\Delta x|x, t)d\Delta x = 1$  and defining the Kramers-Moyal coefficients  $M_n(x, t) = \frac{1}{\tau} \int d\Delta x (\Delta x)^n T(\Delta x|x, t)$  we arrive at the Kramers-Moyal equation

$$\frac{p(x, t + \tau) - p(x, t)}{\tau} = \sum_{n=1}^{\infty} \frac{(-1)^n}{n!} \frac{\partial^n (M_n(x, t)p(x, t))}{\partial x^n} \quad (2.4)$$

Taking the limit  $\tau \rightarrow 0$  all terms in this expansion above  $n = 2$  can be dropped[10] so that

$$\frac{\partial p(x, t)}{\partial t} = -\frac{\partial (M_1(x, t)p(x, t))}{\partial x} + \frac{1}{2} \frac{\partial^2 (M_2(x, t)p(x, t))}{\partial x^2} \quad (2.5)$$

This is known as the Fokker-Planck equation, and governs the evolution of the probability density function for a system evolving under continuous Markovian stochastic dynamics.

## 2.2 Stochastic Calculus

A similar and closely related approach to studying the dynamics of stochastic systems is to describe them with a set of differential equations where deterministic evolution is supplemented with stochastic noise. Consider a system described by a set of variables  $\mathbf{x} = \{x_i(t)\}$ , each of which is governed by a stochastic differential equation of the form

$$dx_i = A_i(\mathbf{x}, t) dt + B_i(\mathbf{x}, t) dW_i \quad (2.6)$$

where  $dW_i$  is a stochastic white noise term representing a Wiener process[7], and which has the properties  $\langle dW_i \rangle = 0$  and  $\langle dW_i^2 \rangle = dt^{1/2}$ . We assume there is no correlation between these noise processes for the different variables, and can rewrite  $dW_i = w(t)dt^{1/2}$  where  $w(t)$  is a number drawn from a normal distribution with zero mean and unit variance. It will be demonstrated in the next section that this description of a stochastic system is equivalent to the use of a generalized Fokker-Planck equation.

If we have a function which depends upon these stochastic variables, we must be careful when considering how this function will change with time. For simplicity consider the case of a continuous function of just one stochastic variable  $x$  and time,  $f(x, t)$ . A small change in  $f$  is given by a Taylor expansion

$$\delta f \approx \frac{\partial f}{\partial t} \delta t + \frac{\partial f}{\partial x} \delta x + \frac{1}{2} \frac{\partial^2 f}{\partial x^2} (\delta x)^2 + \dots \quad (2.7)$$

In the case of non-stochastic variables for small enough changes this could be truncated after the second term, however because  $\delta x$  has a term that goes as  $\delta t^{1/2}$  it is actually necessary to include the third term as well, even to first order. There are various other subtleties involved in performing calculus with stochastic variables, such as requiring  $\delta t$  to be short in terms of the variation in  $x$  and  $f(x, t)$  but long with respect to fluctuations in the stochastic noise, but these will not be explored here. When they are accounted for the result is Itô's Lemma[11]

$$\delta f = \frac{\partial f}{\partial t} \delta t + \frac{\partial f}{\partial x} \delta x + \frac{B(x, t)^2}{2} \frac{\partial^2 f}{\partial x^2} \delta t \quad (2.8)$$

This can then be generalized to functions of more stochastic variables  $f(\mathbf{x}, t)$  such that:

$$\delta f = \frac{\partial f}{\partial t} \delta t + \sum_i \left( \frac{\partial f}{\partial x_i} \delta x_i + \frac{B_i(\mathbf{x}, t)^2}{2} \frac{\partial^2 f}{\partial x_i^2} \delta t \right) \quad (2.9)$$

As a final point worth noting it should be realized that this is just one way of performing calculus with stochastic variables, and other equivalent interpretations are possible but will not be referred to in this report[11].

## 2.3 Stochastic Differential Equations and Relationship with Generalized Fokker-Planck Equations

Systems which have their variables described by stochastic differential equations of the form in equation 2.6 clearly can also be described by a probability density function  $p(\mathbf{x}, t)$ . If we consider an arbitrary continuous function  $f(\mathbf{x})$  with no explicit time dependence, we can construct the average of its time derivative in two ways (remembering that  $\langle dW_i \rangle = 0$ )

$$\left\langle \frac{df(\mathbf{x})}{dt} \right\rangle = \left\langle \sum_i \left( \frac{\partial f}{\partial x_i} A_i(\mathbf{x}, t) + \frac{B_i^2(\mathbf{x}, t)}{2} \frac{\partial^2 f}{\partial x_i^2} \right) \right\rangle = \sum_i \int p(\mathbf{x}, t) \left( \frac{\partial f}{\partial x_i} A_i(\mathbf{x}, t) + \frac{B_i^2(\mathbf{x}, t)}{2} \frac{\partial^2 f}{\partial x_i^2} \right) d\mathbf{x} \quad (2.10)$$

$$\left\langle \frac{df(\mathbf{x})}{dt} \right\rangle = \int f(\mathbf{x}) \frac{\partial p(\mathbf{x}, t)}{\partial t} d\mathbf{x} \quad (2.11)$$

Integrating the first of these by parts and assuming that  $p(\mathbf{x}, t)$  and all its derivative go to zero at infinity we find that

$$\int f(\mathbf{x}) \frac{\partial p(\mathbf{x}, t)}{\partial t} d\mathbf{x} = \int f(\mathbf{x}) \sum_i \left( \frac{1}{2} \frac{\partial^2 (B_i^2(\mathbf{x}, t) p(\mathbf{x}, t))}{\partial x_i^2} - \frac{\partial (A_i(\mathbf{x}, t) p(\mathbf{x}, t))}{\partial x_i} \right) d\mathbf{x} \quad (2.12)$$

However as  $f(\mathbf{x})$  is arbitrary it follows

$$\frac{\partial p(\mathbf{x}, t)}{\partial t} = \sum_i \left( \frac{1}{2} \frac{\partial^2 (B_i^2(\mathbf{x}, t) p(\mathbf{x}, t))}{\partial x_i^2} - \frac{\partial (A_i(\mathbf{x}, t) p(\mathbf{x}, t))}{\partial x_i} \right) \quad (2.13)$$

giving us a partial differential equation governing the evolution of the probability density function. From this we see that we can identify the  $A$  term in equation 2.6 with the first Kramers-Moyal coefficient in equation 2.5  $M_1$  and the second Kramers-Moyal coefficient  $M_2$  with  $\sqrt{B}$ .

## 2.4 Entropy In Stochastic Thermodynamics

Stochastic thermodynamics is really an extension of "Stochastic Energetics" introduced by Sekimoto[12] whereby the quantities of heat and work are meaningfully defined for individual stochastic trajectories and a first-law like energy balance holds. Stochastic thermodynamics takes this a step further by also defining entropy on the level of individual trajectories. To proceed we imagine a system whose evolution is governed by a protocol  $\lambda(t)$  (for an example an external force) and we define a particular trajectory of the system as  $X = \{\mathbf{x}(t) \mid 0 \leq t \leq \tau\}$  and  $\mathcal{P}[X]$  as the probability density for that particular trajectory under the forward protocol. To then construct a quantity which acts as a measure of irreversibility we have to think about what it means for a process to be reversed. For a deterministic system if time is ran forward and the system (and environment) follow a particular path, an application of the time-reversal operator  $\hat{T}$  to all of the system and environmental coordinates (so that positions are unchanged, but velocities are reversed, i.e.  $v \rightarrow -v$ ) and running the protocol in reverse would lead to the system following exactly the reverse trajectory. So we can ask for a given stochastic trajectory  $X$  if we were to apply a time-reversal to all the coordinates of only the system and run the protocol in reverse what is the probability of observing the reverse trajectory, where the reversed trajectory of  $X$  is defined as

$\bar{X} = \{\hat{T}\mathbf{x}(\tau - t) \mid 0 \leq t \leq \tau\}$ . We can then also define a probability density of seeing any given trajectory under the time reversed protocol  $\bar{\lambda}(t) = \lambda(\tau - t)$  as  $\mathcal{P}^R[X]$ . With these definitions in place we then construct the most clear measure of irreversibility for any particular stochastic trajectory and define it as the (dimensionless) entropy production[1]

$$\Delta S[X] = \ln \left( \frac{\mathcal{P}[X]}{\mathcal{P}^R[\bar{X}]} \right) \quad (2.14)$$

Note that with this definition it is perfectly allowable for the entropy to take on negative values, however it will be demonstrated in section that 2.6 that this quantity is always greater than or equal to zero on average. If we consider systems which are described by stochastic differential equations of the form in equation 2.6, we make the definitions

$$\begin{aligned} A_i^{ir}(\mathbf{x}, t) &= \frac{1}{2}(A_i(\mathbf{x}, t) + \varepsilon_i A_i(\hat{T}\mathbf{x}, t)) \\ A_i^{rev}(\mathbf{x}, t) &= \frac{1}{2}(A_i(\mathbf{x}, t) - \varepsilon_i A_i(\hat{T}\mathbf{x}, t)) \\ D_i(\mathbf{x}, t) &= B_i^2(\mathbf{x}, t) \end{aligned} \quad (2.15)$$

where  $\varepsilon_i = \pm 1$  depending on whether the coordinate is even or odd when the time reversal operator is applied, i.e.  $\hat{T}x_i = \varepsilon_i x_i$ . It can then be shown with the use of short time propagators that the small increment in entropy defined in this way along any stochastic trajectory is given by[13]

$$\begin{aligned} d\Delta S_{tot} &= -d(\ln(p(\mathbf{x}))) + \sum_i \left( \frac{A_i^{ir}}{D_i} dx_i - \frac{A_i^{rev} A_i^{ir}}{D_i} dt + \frac{\partial A_i^{ir}}{\partial x_i} dt - \frac{\partial A_i^{rev}}{\partial x_i} dt \right. \\ &\quad \left. - \frac{1}{D_i} \frac{\partial D_i}{\partial x_i} dx_i + \frac{(A_i^{ir} - A_i^{rev})}{D_i} \frac{\partial D_i}{\partial x_i} dt - \frac{\partial^2 D_i}{\partial x_i^2} dt + \frac{1}{D_i} \left( \frac{\partial D_i}{\partial x_i} \right)^2 dt \right) \end{aligned} \quad (2.16)$$

This is actually a completely robust definition for the entropy of any stochastic system, however we are interested particularly in thermodynamic systems when there is a well defined environmental temperature.

## 2.5 Splitting the Entropy into Three Components

It has recently been proposed that the entropy production described in the previous section can be naturally separated into three components[13], each of which is also defined in terms of conditional path probability densities. As such they are also well defined for any system which is described by a set of stochastic differential equations, however they take on particular thermodynamic interpretations when there is an environmental temperature. Before proceeding we define for any particular stochastic path  $X = \{\mathbf{x}(t) \mid 0 \leq t \leq \tau\}$  two further paths,  $X^R = \{\mathbf{x}(\tau - t) \mid 0 \leq t \leq \tau\}$  and  $X^T = \{\hat{T}\mathbf{x}(t) \mid 0 \leq t \leq \tau\}$ . We then also introduce the probability density of any given path X under the adjoint dynamics as  $\mathcal{P}^{ad}[X]$ , where the adjoint dynamics are defined with respect to the forward protocol and are such that if at any time the protocol was frozen and the system allowed to relax, then the stationary state reached under the adjoint dynamics would have the opposite probability current to the stationary state reached under the forward protocol. With these definitions in place three different components  $\Delta S_1$ ,  $\Delta S_2$  and  $\Delta S_3$  are defined as follows

$$\Delta S_1 = \ln \mathcal{P}[X] - \ln \mathcal{P}^{ad,R}[X^R] \quad (2.17)$$

$$\Delta S_2 = \ln \mathcal{P}[X] - \ln \mathcal{P}^{ad}[X^T] \quad (2.18)$$

$$\Delta S_3 = \ln \mathcal{P}^{ad}[X^T] + \ln \mathcal{P}^{ad,R}[X^R] - \ln \mathcal{P}[X] - \ln \mathcal{P}^R[\bar{X}] \quad (2.19)$$

It then follows trivially that  $\Delta S_{tot} = \Delta S_1 + \Delta S_2 + \Delta S_3$ .

In a situation when an environmental temperature is well defined these somewhat obscurely defined quantities can be mapped on to thermodynamic quantities related to the housekeeping and excess heat[14]. In such a situation the change in entropy along a given trajectory can be written as

$$\Delta S_{tot} = \ln \left( \frac{p(\mathbf{x}(0), 0)}{p(\mathbf{x}(\tau), \tau)} \right) + \int_0^\tau d \left( \frac{\Delta Q}{kT_{env}(\mathbf{x}(t), t)} \right) \quad (2.20)$$

such that it is the sum of the change in system entropy and the change in medium entropy. We can then divide the heat transfer to the environment into two components known as the housekeeping heat and the excess heat. The housekeeping heat is defined as the heat required to maintain a non-equilibrium steady state and the excess is the remainder so that  $\Delta Q = \Delta Q_{hk} + \Delta Q_{ex}$ . We then associate  $\Delta S_1$  with the excess heat so that

$$\Delta Q_{ex} = (\Delta S_1 - \Delta S_{sys})kT_{env} \quad (2.21)$$

Although the equivalency of these two quantities is not necessarily obvious, it is clear that the excess heat is related to the relaxation of the system towards a stationary state and that in a stationary state it would equal zero. This is also true of  $\Delta S_1$  as defined in equation 2.18 given the definition of  $X^R$  and the adjoint dynamics so that it will only take on non-zero values in the presence of relaxation. We then separate the housekeeping heat into the generalized housekeeping heat and the transient housekeeping heat so that  $\Delta Q_{hk} = \Delta Q_{hk,G} + \Delta Q_{hk,T}$  and associate  $\Delta S_2$  and  $\Delta S_3$  with each of these quantities so that

$$\Delta Q_{hk,G} = \Delta S_2 kT_{env} \quad (2.22)$$

$$\Delta Q_{hk,T} = \Delta S_3 kT_{env} \quad (2.23)$$

$\Delta S_2$  arises as a result of the absence of detailed balance, and so contributes whenever a system is not in equilibrium, however  $\Delta S_3$  can be shown to only be non-zero when there are system coordinates which are odd with respect to the application of the time-reversal operator. With the three components defined like this it is then possible to show (and will be discussed in the next section) that  $\Delta S_{tot}$ ,  $\Delta S_1$  and  $\Delta S_2$  are always more than or equal to zero on average, however this is not the case for  $\Delta S_3$  which can take on negative average values.

## 2.6 Fluctuation Relations

The fluctuation relations are a number of mathematical relationships which can be derived within the context of stochastic thermodynamics (and also using other formalisms as well)[15] where under certain conditions exact thermodynamic statements can be made about systems arbitrarily far from equilibrium, something which traditionally has been very difficult to achieve. The focus of this section will only be on the two main fluctuation relations explicitly relating to entropy production, however a number of other interesting and closely related results have also been derived [16, 17, 1].

The first important relation is the integral fluctuation relation for the total entropy production, which allows us to demonstrate that entropy defined in this way is consistent with the second law of thermodynamics. If we consider the entropy production over a given time interval and consider the average of the quantity  $\exp \left( -\frac{\Delta S_{tot}}{k} \right)$

over all possible trajectories we find that

$$\left\langle \exp\left(\frac{-\Delta S_{tot}}{k}\right) \right\rangle = \int dX \mathcal{P}[X] \frac{\mathcal{P}^R[\bar{X}]}{\mathcal{P}[X]} = \int d\bar{X} \mathcal{P}^R[\bar{X}] = 1 \quad (2.24)$$

as  $dX$  and  $d\bar{X}$  are defined on the same space. Then using a version of Jensen's inequality[18]

$$\langle \exp A \rangle \geq \exp\langle A \rangle \quad (2.25)$$

it follows that that  $\langle \Delta S_{tot} \rangle \geq 0$ ; a statistical statement of the second law. By the same argument it follows that any quantity which is of the form  $\ln(\mathcal{P}[X]) - \ln(\mathcal{P}^*[X^*])$  will also satisfy an integral fluctuation theorem, where  $X^*$  is some path for which the transformation  $X \rightarrow X^*$  has a Jacobian equal to one and  $\mathcal{P}^*$  is a path probability density for a given choice of dynamics[13]. As defined in equations 2.18 and 2.19  $\Delta S_1$  and  $\Delta S_2$  clearly satisfy these requirements and as such also obey an integral fluctuation theorem. However as there is no way to write  $\Delta S_3$  in this form it does not satisfy the integral fluctuation theorem and can in fact take negative average values.

The second relevant fluctuation relation is known as the detailed fluctuation theorem[1] and gives a much stronger condition on the distribution of entropy production, but only holds true under the correct conditions rather than for all times. The necessary conditions are that the entropy production is taken over a time interval  $0 \leq t \leq \tau$  where the system probability density function is the same at the beginning and at the end, and that the protocol is time symmetric such that  $\lambda(t) = \lambda(\tau - t)$ . When these conditions are met (for example with a non-equilibrium steady state, or over a certain interval for an oscillatory non-equilibrium state) the following relationship holds

$$\frac{P(\Delta S_{tot})}{P(-\Delta S_{tot})} = \exp\left(\frac{\Delta S_{tot}}{k}\right) \quad (2.26)$$

relating the probability of seeing a particular value of entropy production to the probability of seeing the negative of that value.

## Chapter 3

# Brownian Particle in a Non-Isothermal Heat Bath

In this chapter the particular system which is the main focus of this report is introduced; a Brownian particle in a heat bath with a spatially and temporally varying temperature profile. In the first section we will look at the basic equations which govern the dynamics of this system and derive some simple results which will be of use later on. In the second section we derive a general expression for the average rate of entropy production for this system, before going on to calculate an approximate probability density function in section 3.3 and then obtaining an expression for the average rate of entropy production and all of the individual components using the approximately obtained PDF.

### 3.1 Basic Description of System

Building on earlier work which looked at the case where the temperature profile only varies spatially[13], we consider a Brownian particle in a heat bath which has a temperature profile given by  $T_r(x, t)$  and is held in place with a confining force  $F(x)$ . The dynamics of this system are governed by the Langevin equation which gives the evolution of the particle's velocity[10]

$$dv = -\gamma v dt + \frac{F(x)}{m} dt + \sqrt{\frac{2kT_r(x, t)\gamma}{m}} dW \quad (3.1)$$

along with its position which is simply described by  $dx = v dt$ . It is worth noting that in most studies of a Brownian particle in a heat bath which is driven in some way from equilibrium the overdamped Langevin equation is employed, where the velocity distribution is taken to relax instantaneously so that only the position coordinate is accounted for and which evolves according to[5]

$$dx = \frac{F(x)}{m\gamma} dt + \sqrt{\frac{2kT_r}{m\gamma}} dW \quad (3.2)$$

In the case of a stationary spatially varying temperature profile this leads to zero entropy production for all trajectories[13] and so to provide a more satisfactory description of entropy production in this system we have to use a description in full phase space. From equation 2.16 it follows that the incremental dimensionless entropy

change along a given stochastic trajectory is given by

$$d\Delta S_{tot} = -d(\ln p(\mathbf{x}, t)) - \frac{mv}{kT_r} dv + \frac{vF}{kT_r} dt - \gamma dt \quad (3.3)$$

We then note that using the rules of Itô calculus that  $d\left(\frac{mv^2}{2}\right) = mv dv + kT_r \gamma dt$ , and also that  $v dt = dx$  so that this can be re-written as

$$d\Delta S_{tot} = -d(\ln p(\mathbf{x}, t)) - \frac{1}{kT_r} d\left(\frac{mv^2}{2}\right) + \frac{F(x)}{kT_r} dx \quad (3.4)$$

Written in this form it is more clearly demonstrated that the change in medium entropy is equivalent to a heat transfer between the system and environment, i.e.  $d\Delta S_{med} = \frac{d\Delta Q}{kT_r}$ . The Fokker-Planck equation which corresponds to the full phase description, known as the Kramers equation[10], is then

$$\frac{\partial p(x, v, t)}{\partial t} = -v \frac{\partial p(x, v, t)}{\partial x} - \frac{\partial}{\partial v} \left[ \left( \frac{F(x)}{m} - \gamma v \right) p(x, v, t) \right] - \frac{kT_r(x, t) \gamma}{m} \frac{\partial^2 p(x, v, t)}{\partial v^2} \quad (3.5)$$

which can be re-written in another useful form as

$$\frac{\partial p(x, v, t)}{\partial t} + v \frac{\partial p(x, v, t)}{\partial x} + \frac{F}{m} \frac{\partial p(x, v, t)}{\partial v} = - \frac{\partial J_v^{ir}}{\partial v} \quad (3.6)$$

where we define  $J_v^{ir} = -\gamma v p(x, v, t) - \frac{kT_r(x, t) \gamma}{m} \frac{\partial p(x, v, t)}{\partial v}$ . This can be thought of in a way as a special case of the Boltzmann equation[19].

We now define certain quantities and derive some equations which will be useful when we come to model the probability density function of the system and calculate the average entropy production. As a starting point we define  $\rho = \int p(x, v, t) dv$ ,  $\rho \bar{v} = \int p(x, v, t) v dv$  and generalize so that  $\rho \bar{v}^n = \int p(x, v, t) v^n dv$ . We then integrate equation 3.6 over  $v$ :

$$\frac{\partial}{\partial t} \int p dv + \frac{\partial}{\partial x} \int pv dv + \frac{F}{m} \int \frac{\partial p}{\partial v} dv = - \int \frac{\partial J_v^{ir}}{\partial v} dv \quad (3.7)$$

which assuming  $p$  and  $\frac{\partial p}{\partial v}$  go to zero at the boundaries gives a continuity equation

$$\frac{\partial \rho}{\partial t} + \frac{\partial(\rho \bar{v})}{\partial x} = 0 \quad (3.8)$$

Multiplying equation 3.6 by  $v$  and again integrating over  $v$  then gives

$$\frac{\partial(\rho \bar{v})}{\partial t} + \frac{\partial(\rho \bar{v}^2)}{\partial x} - \frac{F}{m} \rho = -\gamma \bar{v} \rho \quad (3.9)$$

Defining a system temperature  $T$  (itself also a function of position and time) in the most natural way so that

$$\frac{kT}{m} = \bar{v}^2 - \bar{v}^2 \quad (3.10)$$

then allows us to re-write equation 3.9 as

$$\rho \frac{\partial \bar{v}}{\partial t} + \frac{k}{m} \frac{\partial(\rho T)}{\partial x} + \rho \bar{v} \frac{\partial \bar{v}}{\partial x} - \frac{F}{m} \rho = -\gamma \rho \bar{v} \quad (3.11)$$

We note that in the case of a stationary temperature profile the continuity equation requires that  $\bar{v} = 0$  and so this reduces to

$$k \frac{\partial(\rho T)}{\partial x} = F \rho \quad (3.12)$$

which is compatible with  $\rho \propto \frac{1}{T} \exp\left(\int_0^x \frac{F(x')}{kT(x')} dx'\right)$ , the solution to the Fokker-Planck equation corresponding to the stationary overdamped Langevin equation (provided that T is taken as  $T_r$ ).

We then proceed by employing a model where  $p(x, v, t) = f(1 + \phi)$ , where f is defined as

$$f = \rho \left(\frac{m}{2\pi kT_r}\right)^{1/2} \exp\left(\frac{-m(v - \bar{v})^2}{2kT_r}\right) \quad (3.13)$$

and we shall look to approximate  $\phi$  in section 3.3, so really this amounts to an expansion around the Maxwell local equilibrium function[19]. Defined in this way and using the definitions for  $\rho$  and  $\bar{v}$  it is then straightforward to show that

$$\int dv f \phi = 0 \quad (3.14)$$

and

$$\int dv v f \phi = 0 \quad (3.15)$$

which will be made use of in the next section where an expression for the average rate of entropy production will be obtained.

## 3.2 General Expression for Average Entropy Production Rate

The average total rate of (dimensionless) entropy production in a system obeying a set of stochastic differential equations can be obtained by averaging over equation 2.16 and is given by[13]

$$\frac{d\langle \Delta S_{tot} \rangle}{dt} = \sum_i \int d\mathbf{x} \frac{J_i^{ir}(\mathbf{x}, t)^2}{p(\mathbf{x}, t) D_i(\mathbf{x}, t)} \quad (3.16)$$

where  $J_i^{ir}$  is defined as

$$J_i^{ir}(\mathbf{x}, t) = A_i^{ir}(\mathbf{x}, t)p(\mathbf{x}, t) - \frac{\partial(D_i(\mathbf{x}, t)p(\mathbf{x}, t))}{\partial x_i} \quad (3.17)$$

For the system being considered this reduces to

$$\frac{d\langle \Delta S_{tot} \rangle}{dt} = \int dx dv \frac{m}{kT_r \gamma p} (J_v^{ir})^2 \quad (3.18)$$

where  $J_v^{ir}$  has already been introduced in the previous section as  $J_v^{ir} = -\gamma v p - \frac{kT_r \gamma}{m} \frac{\partial p}{\partial v}$ . This can be re-written as

$$J_v^{ir} = -\gamma v f - \gamma v f \phi - \frac{kT_r \gamma}{m} \frac{\partial f}{\partial v} - \frac{kT_r \gamma}{m} \frac{\partial(f\phi)}{\partial v} \quad (3.19)$$

which using  $\frac{\partial f}{\partial v} = -\frac{m}{kT_r} (v - \bar{v}) f$  reduces to

$$J_v^{ir} = -\gamma \bar{v} p - \frac{kT_r \gamma}{m} f \frac{\partial \phi}{\partial v} \quad (3.20)$$

With this result we can look to obtain an expression for the spatial density of the rate of entropy production by carrying out the integration of equation 3.18 over velocity only

$$\int dv \frac{m}{kT_r \gamma p} (J_v^{ir})^2 = \int dv \frac{m \gamma p \bar{v}^2}{kT_r} + 2 \int dv \bar{v} \gamma f \frac{\partial \phi}{\partial v} + \int dv \frac{kT_r \gamma}{pm} f^2 \left( \frac{\partial \phi}{\partial v} \right)^2 \quad (3.21)$$

Now using equations 3.14 and 3.15 and re-writing  $f \frac{\partial \phi}{\partial v} = \frac{\partial(f\phi)}{\partial v} - \phi \frac{\partial f}{\partial v}$  this can be simplified so that the spatial density of the rate of entropy production is given by

$$\int dv \frac{m}{kT_r \gamma p} (J_v^{ir})^2 = \frac{m \gamma \rho \bar{v}^2}{kT_r} + \int dv \frac{1}{1 + \phi} \frac{kT_r \gamma}{m} f \left( \frac{\partial \phi}{\partial v} \right)^2 \quad (3.22)$$

We will use this expression in section 3.4 to calculate an approximate expression for the average rate of entropy production for this system once we have found an appropriate approximation for  $\phi$ .

### 3.3 Calculation of an Approximate PDF

Using the model for the probability density function of  $p = f(1 + \phi)$  where  $f$  was defined in section 3.1 we proceed by making a power series expansion of the second term in  $\frac{1}{\gamma}$

$$f\phi = f \left( \frac{1}{\gamma} \phi_1 + \frac{1}{\gamma^2} \phi_2 + \dots \right) \quad (3.23)$$

as  $f$  has no explicit dependence on  $\gamma$ . We then gather all terms in the Kramers equation of order zero in  $\frac{1}{\gamma}$  so that we are really looking for a solution in the vicinity of the overdamped limit, which should lead to something similar to linear irreversible thermodynamics (we also assume that  $\bar{v} \propto \frac{1}{\gamma}$ ). Doing this we are left with

$$\frac{\partial f}{\partial t} + v \frac{\partial f}{\partial x} + \left( \frac{F}{m} - \gamma \bar{v} \right) \frac{\partial f}{\partial v} = \frac{kT_r \gamma}{m} \frac{\partial}{\partial v} \left( f \frac{\partial \left( \frac{1}{\gamma} \phi_1 \right)}{\partial v} \right) \quad (3.24)$$

where we have made use of eq 3.20. Rather than trying to solve this partial differential equation directly we instead employ a variational approach whereby we maximize a functional which approximately corresponds to the rate of entropy production. From now on we shall define  $\phi = \frac{1}{\gamma} \phi_1$  and we then note that the previous equation is of the form

$$Z = \hat{L}\phi \quad (3.25)$$

where  $\hat{L}$  is a linear operator. Defining the bilinear expression

$$(A, B) = \int dv AB \quad (3.26)$$

we then construct a functional  $J[\tilde{\phi}]$  which is to be extremized over trial solutions  $\tilde{\phi}$  satisfying the necessary constraints

$$J[\tilde{\phi}] = (\tilde{\phi}, \hat{L}\tilde{\phi}) - 2(\tilde{\phi}, Z) \quad (3.27)$$

The first term can be written as

$$(\tilde{\phi}, \hat{L}\tilde{\phi}) = \int dv \tilde{\phi} \frac{kT_r \gamma}{m} \frac{\partial}{\partial v} \left( f \frac{\partial \tilde{\phi}}{\partial v} \right) \quad (3.28)$$

which upon integrating by parts gives

$$(\tilde{\phi}, \hat{L}\tilde{\phi}) = - \int dv \frac{kT_r \gamma}{m} f \left( \frac{\partial \tilde{\phi}}{\partial v} \right)^2 \quad (3.29)$$

assuming that  $\tilde{\phi}$  does not increase exponentially or faster at the boundaries. We then note that with  $\hat{L}$  defined in this way it is easy to demonstrate that for two functions of this kind  $\alpha(v)$  and  $\beta(v)$  that

$$(\hat{L}\alpha, \beta) = (\alpha, \hat{L}\beta) \quad (3.30)$$

It can then be shown that extremizing  $J[\tilde{\phi}]$  will give the optimal solution  $\phi$  by defining  $\tilde{\phi} = \phi + \eta$  so that

$$\begin{aligned} J[\phi + \eta] &= (\phi + \eta, \hat{L}(\phi + \eta)) - 2(\phi + \eta, Z) \\ &= (\phi, \hat{L}\phi) + (\phi, \hat{L}\eta) + (\eta, \hat{L}\phi) + (\eta, \hat{L}\eta) - 2(\phi, Z) - 2(\eta, Z) \\ &= J[\phi] + (\hat{L}\phi, \eta) + (\eta, \hat{L}\phi) + (\eta, \hat{L}\eta) - 2(\eta, Z) \\ &= J[\phi] + (\eta, \hat{L}\eta) \end{aligned} \quad (3.31)$$

Now looking at equation 3.29 it is clear that  $(\eta, \hat{L}\eta)$  is negative which this means that the optimal solution of  $\tilde{\phi} = \phi$  is found by maximizing the functional  $J[\tilde{\phi}]$ . We note that the functional  $J[\tilde{\phi}]$  for the optimal solution is equal to

$$J[\phi] = -(\phi, \hat{L}\phi) = \int dv \frac{kT_r \gamma}{m} f \left( \frac{\partial \phi}{\partial v} \right)^2 \quad (3.32)$$

which comparing with equation 3.22 can be seen to be the rate of entropy production to first order in  $\frac{1}{\gamma}$  in the approximation that  $\bar{v} = 0$ . So the maximization of this functional is something like the application of a maximum entropy production principle[19].

We now examine the second term in the functional and write

$$(\tilde{\phi}, Z) = \int dv \tilde{\phi} \frac{\partial f}{\partial t} + \int dv \tilde{\phi} v \frac{\partial f}{\partial x} + \int dv \tilde{\phi} \left( \frac{F}{m} - \gamma \bar{v} \right) \frac{\partial f}{\partial v} \quad (3.33)$$

Looking at the first term here and using the earlier definition of  $f$  as well as assuming that the earlier results  $\int dv f \phi = 0$  and  $\int dv v f \phi = 0$  hold for each term in the power series expansion of  $\phi$  performed in equation 3.23 we can write

$$\begin{aligned} \int dv \tilde{\phi} \frac{\partial f}{\partial t} &= \int dv \tilde{\phi} \left( \frac{\partial \rho}{\partial t} \frac{f}{\rho} - \frac{f}{2T_r} \frac{\partial T_r}{\partial t} + f \left( \frac{m(v - \bar{v})}{kT_r} \frac{\partial \bar{v}}{\partial t} + \frac{m(v - \bar{v})^2}{2kT_r^2} \frac{\partial T_r}{\partial t} \right) \right) \\ &= \int dv \tilde{\phi} f \left( \frac{m(v - \bar{v})^2}{2kT_r^2} \frac{\partial T_r}{\partial t} \right) \end{aligned} \quad (3.34)$$

Similarly for the second term

$$\begin{aligned} \int dv \tilde{\phi} v \frac{\partial f}{\partial v} &= \int dv \tilde{\phi} v \left( \frac{\partial \rho}{\partial x} \frac{f}{\rho} - \frac{f}{2T_r} \frac{\partial T_r}{\partial x} + f \left( \frac{m(v - \bar{v})}{kT_r} \frac{\partial \bar{v}}{\partial x} + \frac{m(v - \bar{v})^2}{2kT_r^2} \frac{\partial T_r}{\partial x} \right) \right) \\ &= \int dv \tilde{\phi} v f \left( \frac{mv}{kT_r} \frac{\partial \bar{v}}{\partial x} + \frac{m(v - \bar{v})^2}{2kT_r^2} \frac{\partial T_r}{\partial x} \right) \end{aligned} \quad (3.35)$$

and clearly the third term is equal to zero. This means that we are maximizing the functional

$$J[\tilde{\phi}] = - \int dv \frac{kT_r \gamma}{m} f \left( \frac{\partial \tilde{\phi}}{\partial v} \right)^2 - \frac{m}{kT_r^2} \frac{\partial T_r}{\partial t} \int dv \tilde{\phi} f (v - \bar{v})^2 - 2 \int dv \tilde{\phi} f v \left( \frac{mv}{kT_r} \frac{\partial \bar{v}}{\partial x} + \frac{m(v - \bar{v})^2}{2kT_r^2} \frac{\partial T_r}{\partial x} \right) \quad (3.36)$$

subject to the conditions that  $\int dv \tilde{\phi} f = 0$  and  $\int dv \tilde{\phi} f v = 0$ . We then define

$$h(\tilde{\phi}, \tilde{\phi}', v) = - \frac{kT_r \gamma}{m} f \left( \tilde{\phi}' \right)^2 - \frac{m}{kT_r^2} \frac{\partial T_r}{\partial t} \tilde{\phi} f (v - \bar{v})^2 - 2 \tilde{\phi} f v \left( \frac{m(v - \bar{v})}{kT_r} \frac{\partial \bar{v}}{\partial x} + \frac{m(v - \bar{v})^2}{2kT_r^2} \frac{\partial T_r}{\partial x} \right) + \lambda_1 \tilde{\phi} f + \lambda_2 \tilde{\phi} f v \quad (3.37)$$

where  $\tilde{\phi}' = \frac{\partial \tilde{\phi}}{\partial v}$  and  $\lambda_1$  and  $\lambda_2$  are Lagrange multipliers. To get the optimal  $\tilde{\phi}$  we use the Euler-Lagrange equation[20]

$$\frac{d}{dv} \left( \frac{\partial h}{\partial \tilde{\phi}'} \right) = \frac{\partial h}{\partial \tilde{\phi}} \quad (3.38)$$

which gives

$$- \frac{2kT_r \gamma}{m} \frac{\partial}{\partial v} \left( f \frac{\partial \tilde{\phi}}{\partial v} \right) = - \frac{m}{kT_r^2} \frac{\partial T_r}{\partial t} f (v - \bar{v})^2 - 2v f \left( \frac{m(v - \bar{v})}{kT_r} \frac{\partial \bar{v}}{\partial x} + \frac{m(v - \bar{v})^2}{2kT_r^2} \frac{\partial T_r}{\partial x} \right) + \lambda_1 f + \lambda_2 v f \quad (3.39)$$

We can then re-write the left hand side as

$$- \frac{2kT_r \gamma}{m} \frac{\partial}{\partial v} \left( f \frac{\partial \tilde{\phi}}{\partial v} \right) = - \frac{2kT_r \gamma}{m} \left( \frac{-m(v - \bar{v})}{kT_r} \frac{\partial \tilde{\phi}}{\partial v} f + f \frac{\partial^2 \tilde{\phi}}{\partial v^2} \right) \quad (3.40)$$

and reverting to the notation  $\tilde{\phi} = \phi$  we try a trial solution of  $\phi = \phi_0 + a(v - \bar{v}) + b(v - \bar{v})^2 + c(v - \bar{v})^3$ . For notational convenience define  $z = v - \bar{v}$  so that substitution into equation 3.39/3.40 gives

$$- \frac{2kT_r \gamma}{m} \left( - \frac{mz}{kT_r} (a + 2bz + 2cz^2) + 2b + 6cz \right) = - \frac{m}{kT_r^2} \frac{\partial T_r}{\partial t} z^2 - 2(z + \bar{v}) \left( \frac{mz}{kT_r} \frac{\partial \bar{v}}{\partial x} + \frac{mz^2}{2kT_r^2} \frac{\partial T_r}{\partial x} \right) + \lambda_1 + \lambda_2 (z + \bar{v}) \quad (3.41)$$

Comparing coefficients of  $z$  then gives us four equations:

$$\lambda_1 + \lambda_2 \bar{v} = - \frac{4kT_r \gamma}{m} b \quad (3.42)$$

$$- \frac{2\bar{v}m}{kT_r} \frac{\partial \bar{v}}{\partial x} + \lambda_2 = - \frac{2kT_r \gamma}{m} \left( -a \frac{m}{kT_r} + 6c \right) \quad (3.43)$$

$$- \frac{m}{kT_r} \left( \frac{1}{T_r} \frac{\partial T_r}{\partial t} + 2 \frac{\partial \bar{v}}{\partial x} + \frac{\bar{v}}{T_r} \frac{\partial T_r}{\partial x} \right) = 4\gamma b \quad (3.44)$$

$$- \frac{m}{kT_r^2} \frac{\partial T_r}{\partial x} = 6\gamma c \quad (3.45)$$

We can immediately read off from the last two that  $b = -\frac{m}{4kT_r\gamma} \left( \frac{1}{T_r} \frac{\partial T_r}{\partial t} + 2\frac{\partial \bar{v}}{\partial x} + \frac{\bar{v}}{T_r} \frac{\partial T_r}{\partial x} \right)$  and  $c = -\frac{m}{6\gamma kT_r^2} \frac{\partial T_r}{\partial x}$ . To get the other coefficients we first have to impose

$$\begin{aligned} 0 &= \int dv \phi f \\ &= \int dz (\phi_0 + az + bz^2 + cz^3) f \\ &= \int dz (\phi_0 + bz^2) f \end{aligned} \quad (3.46)$$

such that that  $\phi_0 + \frac{bkT_r}{m} = 0$ . We then impose the second constraint

$$\begin{aligned} 0 &= \int dv \phi f v \\ &= \int dz (z + \bar{v})(\phi_0 + az + bz^2 + cz^3) f \\ &= \int dz z(az + cz^3) f \end{aligned} \quad (3.47)$$

such that  $a = -\frac{3ckT_r}{m}$ . Bringing this all together leaves us with

$$\begin{aligned} \phi_0 &= \frac{1}{4\gamma} \left( \frac{1}{T_r} \frac{\partial T_r}{\partial t} + 2\frac{\partial \bar{v}}{\partial x} + \frac{\bar{v}}{T_r} \frac{\partial T_r}{\partial x} \right) \\ a &= \frac{1}{2\gamma T_r} \frac{\partial T_r}{\partial x} \\ b &= -\frac{m}{4kT_r\gamma} \left( \frac{1}{T_r} \frac{\partial T_r}{\partial t} + 2\frac{\partial \bar{v}}{\partial x} + \frac{\bar{v}}{T_r} \frac{\partial T_r}{\partial x} \right) \\ c &= -\frac{m}{6\gamma kT_r^2} \frac{\partial T_r}{\partial x} \end{aligned} \quad (3.48)$$

We now just need expressions for  $\rho$  and  $\bar{v}$  and our approximate PDF is complete. We start off by noting that we can now evaluate  $\overline{\rho v^2}$

$$\overline{\rho v^2} = \int dv p v^2 = \rho \int dv \left( \frac{m}{2\pi kT_r} \right)^{1/2} \exp\left(-\frac{m(v-\bar{v})^2}{2kT_r}\right) v^2 (1 + \phi_0 + a(v-\bar{v}) + b(v-\bar{v})^2 + c(v-\bar{v})^3) \quad (3.49)$$

so that

$$\overline{v^2} = \frac{kT_r}{m} (1 + \phi_0 + 2\bar{v}a + b\bar{v}^2) + \frac{3k^2T_r^2}{m^2} (b + 2\bar{v}c) + \bar{v}^2(1 + \phi_0) \quad (3.50)$$

We now have  $\overline{v^2}$  in terms of known quantities and  $\bar{v}$ , so that equations 3.8 and 3.9 reduce to two differential equations for two unknowns  $\rho$  and  $\bar{v}$ . We will investigate obtaining numerical solutions to these equations exactly in section 4.3, but for the rest of the analytic work we will employ a stationary approximation where  $\bar{v} = 0$  and

$$\rho \propto \frac{1}{T_r(x, t)} \exp\left(\int dx' \frac{F(x')}{kT_r(x', t)}\right) \quad (3.51)$$

where actually once the temperature profile is defined we will employ a time average to make  $\rho$  time-independent, which we shall call  $\rho_{st}$ . This approximation should be reasonable for large  $\gamma$  and for temperature profiles which do not vary too quickly in time. Justification for using  $T_r$  rather than  $T$  for the stationary approximation comes

from noting that equation 3.50 implies that

$$\frac{kT}{m} = \frac{kT_r}{m} (1 + \phi_0 + 2\bar{v}a + b\bar{v}^2) + \frac{3k^2T_r^2}{m^2} (b + 2\bar{v}c) + \bar{v}\phi_0 \quad (3.52)$$

which in the case of a stationary temperature profile when  $\phi_0 = 0$ ,  $b = 0$  and  $\bar{v} = 0$  reduces to  $T = T_r$ , and in the non-stationary case to first order in  $\frac{1}{\gamma}$  becomes

$$(T - T_r) \approx \phi_0 T_r + \frac{3kT_r^2}{m} b \quad (3.53)$$

using the expressions just found for  $\phi_0$  and  $b$  this then gives

$$(T - T_r) \approx \frac{-1}{2\gamma} \frac{\partial T_r}{\partial t} \quad (3.54)$$

so that for large enough gamma and slow variations in the environmental temperature the difference is small. The final expression for the approximate probability density function is then given by

$$p(x, v, t) = \rho_{st} \left( \frac{m}{2\pi kT_r} \right)^{1/2} \exp \left( \frac{-mv^2}{2kT_r} \right) (1 + \phi_0 + av + bv^2 + cv^3) \quad (3.55)$$

### 3.4 Approximate Rate of Entropy Production

In this section we will use the probability density function obtained in the previous section to obtain approximate expressions for the average rate of total entropy production as well as the rate of production for each of the three components introduced in section 2.5. We start from equation 3.22 and take the expression to first order in  $\frac{1}{\gamma}$  only so that

$$\begin{aligned} \frac{d\langle \Delta S_{tot} \rangle}{dt} &= \int dx dv \frac{kT_r \gamma}{m} f \left( \frac{\partial \phi}{\partial v} \right)^2 \\ &= \int dx dz \frac{kT_r \gamma}{m} \rho \left( \frac{m}{2\pi kT_r} \right)^{1/2} \exp \left( -\frac{-mz^2}{2kT_r} \right) (a^2 + 4b^2 z^2 + 9c^2 z^4 + 6acz^2) \\ &= \int dx \frac{kT_r \gamma}{m} \rho \left( 18c^2 \left( \frac{kT_r}{m} \right)^2 + 4b^2 \frac{kT_r}{m} \right) \end{aligned} \quad (3.56)$$

In the approximation that  $\rho \approx \rho_{st}$  and  $\bar{v} = 0$  so that  $b = \frac{-m}{4k\gamma T_r^2} \frac{\partial T_r}{\partial t}$  this then gives

$$\frac{d\langle \Delta S_{tot} \rangle}{dt} = \int dx \frac{k}{2\gamma T_r} \rho_{st} \left[ \left( \frac{\partial T_r}{\partial x} \right)^2 + \frac{m}{2kT_r} \left( \frac{\partial T_r}{\partial t} \right)^2 \right] \quad (3.57)$$

In the case where the temperature profile is stationary this matches the case studied by Stolovitsky[21]. We also see in the limit  $\gamma \rightarrow \infty$  this goes to zero, in agreement with what is obtained from the overdamped Langevin equation. Although it may seem unintuitive that a larger value of  $\gamma$  and hence a stronger coupling between the system and environment should decrease the rate of entropy production, this can be understood by realizing that with large  $\gamma$  there is a much lower spatial transport of heat despite larger transfers of heat to and from the environment. We can then use expressions derived by Ford and Spinney[13] for the average rate of production

of the three separate components. For this system they are given by

$$\frac{d\langle\Delta S_1\rangle}{dt} = \int dx dv \frac{mp}{kT_r\gamma} \left( \frac{J_v^{ir}}{p} - \frac{J_v^{ir,st}}{p_{st}} \right)^2 \quad (3.58)$$

$$\frac{d\langle\Delta S_2\rangle}{dt} = \int dx dv \frac{mp}{kT_r\gamma} \left( \frac{J_v^{ir,st}(\hat{T}\mathbf{x})}{p_{st}(\hat{T}\mathbf{x})} \right)^2 \quad (3.59)$$

$$\frac{d\langle\Delta S_3\rangle}{dt} = \int dx dv \frac{\partial p}{\partial t} \ln \left( \frac{p_{st}(\mathbf{x})}{p_{st}(\hat{T}\mathbf{x})} \right) \quad (3.60)$$

where  $p_{st}$  is defined as the probability distribution the system would settle down to if the driving were frozen and the system allowed to relax, so that with the model being used this gives  $p_{st} = \rho_{st} \left( \frac{m}{2\pi kT_r} \right)^{1/2} \exp \left( \frac{-mv^2}{2kT_r} \right) (1 + av + cv^3)$ .  $J_v^{ir,st}$  is defined in the same way as  $J_v^{ir}$  but with  $p$  replaced by  $p_{st}$ . Again in the approximation that  $\bar{v} = 0$  and  $\rho = \rho_{st}$  using equation 3.20 we can write  $J_v^{ir} = \frac{-kT_r\gamma}{m} f \frac{\partial \phi}{\partial v}$ , so that

$$\frac{d\langle\Delta S_1\rangle}{dt} = \int dx dv f(1 + \phi) \frac{kT_r\gamma}{m} \left( \frac{1}{1 + \phi_{st}} \frac{\partial \phi_{st}}{\partial v} - \frac{1}{1 + \phi} \frac{\partial \phi}{\partial v} \right)^2 \quad (3.61)$$

where  $\phi_{st}$  is defined as  $(1 + av + cv^3)$ . Taking this expression to first order in  $\frac{1}{\gamma}$  leaves

$$\frac{d\langle\Delta S_1\rangle}{dt} = \int dx dv \rho_{st} \left( \frac{m}{2\pi kT_r} \right)^{1/2} \exp \left( \frac{-mv^2}{2kT_r} \right) \frac{kT_r\gamma}{m} (-2bv)^2 \quad (3.62)$$

which can be integrated over  $v$  to obtain

$$\frac{d\langle\Delta S_1\rangle}{dt} = \int dx \rho \left( \frac{\partial T_r}{\partial t} \right)^2 \frac{1}{4\gamma T_r^2} \quad (3.63)$$

This is equal to the second term in the expression for the total rate of entropy production given in equation 3.57, and as expected for  $\Delta S_1$  only has a non-zero average when the temperature profile is changing, and hence when the system is relaxing. Equation 3.59 then becomes

$$\frac{d\langle\Delta S_2\rangle}{dt} = \int dx dv f(1 + \phi) \frac{kT_r\gamma}{m} \left( \frac{a + 3cv^2}{1 - av - cv^3} \right)^2 \quad (3.64)$$

as clearly  $J_v^{ir,st}(\mathbf{x}, t) = J_v^{ir,st}(\hat{T}\mathbf{x}, t)$ . Again to first order in  $\frac{1}{\gamma}$  this then gives

$$\begin{aligned} \frac{d\langle\Delta S_2\rangle}{dt} &= \int dx dv f \frac{kT_r\gamma}{m} (a + 3cv^2)^2 \\ &= \int dx \rho_{st} \frac{kT_r\gamma}{m} \left( a^2 + 3ac \left( \frac{2kT_r}{m} \right) + \frac{27}{4} c^2 \left( \frac{2kT_r}{m} \right)^2 \right) \\ &= \int dx \rho_{st} \frac{k}{2m\gamma T_r} \left( \frac{\partial T_r}{\partial x} \right)^2 \end{aligned} \quad (3.65)$$

which corresponds to the first term in equation 3.57. This means that to first order in  $\frac{1}{\gamma}$  there is no contribution to the total average entropy production from  $\Delta S_3$ , which can be shown explicitly by noting that  $\ln \left( \frac{1+av+cv^3}{1-av-cv^3} \right) \approx$

$2av + 2cv^3$  so that equation 3.60 becomes

$$\frac{d\langle\Delta S_3\rangle}{dt} = \int dx dv \frac{\partial p}{\partial t} (2av + 2cv^3) = \int dx \left( 2a \frac{\partial(\rho\bar{v})}{\partial t} + 2c \frac{\partial(\rho\bar{v}^3)}{\partial t} \right) \quad (3.66)$$

We've been using the approximation  $\bar{v} = 0$  and when we evaluate  $\overline{\rho v^3}$  all terms will be of order  $\frac{1}{\gamma}$  such that the second term in equation 3.66 is of order  $\frac{1}{\gamma^2}$ , so that to first order  $\frac{d\langle\Delta S_3\rangle}{dt} = 0$ .

## Chapter 4

# Sinusoidally Varying Quadratic Temperature Profile

In this section a specific temperature profile is chosen so that  $T_r(x, t) = T_0 \left( 1 + \frac{\kappa_T(t)x^2}{2kT_0} \right)$  with  $\kappa_T(t) = \kappa_T(0) + B\sin(\omega t)$  and studied in detail, comparing the analytically predicted average entropy production to the average production over a large number of simulated stochastic trajectories. This is then also done for each of the three components of entropy production individually as well as looking at their distributions and attempting to demonstrate their adherence to the relevant fluctuation relations. Although a temperature profile of this form would be physically difficult to impose on a system, for the purposes of a theoretical study it is useful for its simplicity and for the fact that it allows an analytic solution for  $\rho_{st}$  to be obtained. The confining force is taken to be a simple harmonic force  $F(x) = -\kappa x$

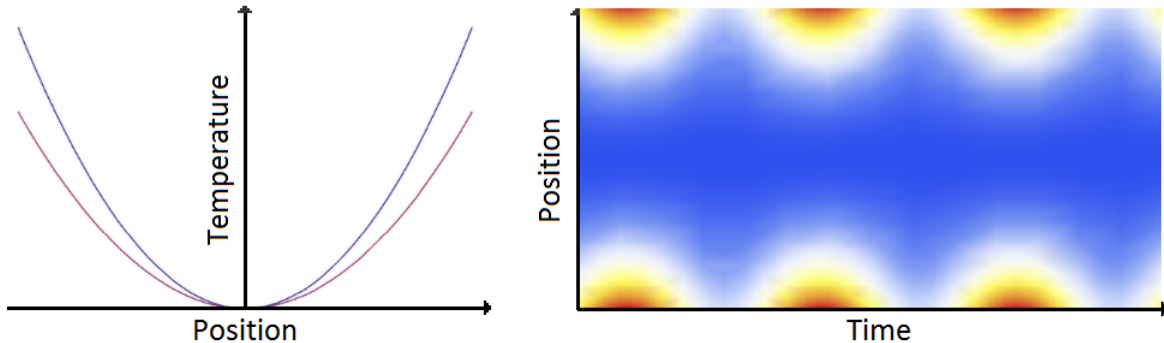


Figure 4.1: The temperature profile of the heat bath being studied. The first image shows the temperature as a function of position at two different times, whilst the second shows a density plot of the profile as a function of position at time with the hotter regions (red) compared to the cooler regions (blue).

The first step was to choose an appropriate selection of parameters. Whilst not an obviously important step other than to make sure that the  $\gamma$  being used is large enough so that the approximations made can be justified, with hindsight a lot of time could have been saved with a more thorough investigation earlier on in the project of how the choice of parameters can affect the results obtained from simulating the stochastic trajectories of the particle. In particular experience has found that when the dimensionless entropy production is very small (lower than about  $10^{-4}$  for a couple of temperature cycles) that a very large number of timesteps are required to obtain a stochastic average which does not change when you use an even larger number of timesteps (for a

given time interval), as well as to obtain an average which is not too noisy. The values used for the majority of this project were chosen, largely for simplicity, to be  $\kappa = 1, m = 1, T_0 = 1, k = 1, \kappa_T(0) = 0.5, B = 0.2$  (or zero when the stationary profile is looked at),  $\omega = 8$  and with  $\gamma$  being probed to find the appropriate value given the approximations used. Unless otherwise specified it should be assumed that these were the parameters being used.

## 4.1 Stationary Temperature Profile

We initially looked at the stationary quadratic profile (i.e.  $B = 0$ ) to investigate how  $\gamma$  affects the agreement between the analytic and stochastically obtained rates of entropy production. We start by using equation 3.51 to obtain an expression for  $\rho_{st}$ .

$$\rho_{st} \propto \frac{1}{T_0 \left(1 + \frac{\kappa_T(0)x^2}{2kT_0}\right)} \exp\left(\int_0^x dx' \frac{-\kappa x'}{kT_0 \left(1 + \frac{\kappa_T(0)x'^2}{2kT_0}\right)}\right) \quad (4.1)$$

which when evaluated and properly normalized gives

$$\rho_{st} = \left(\frac{\kappa_T(0)}{2\pi kT_0}\right)^{1/2} \frac{\Gamma\left(1 + \frac{\kappa}{\kappa_T(0)}\right)}{\Gamma\left(0.5 + \frac{\kappa}{\kappa_T(0)}\right)} \left[1 + \frac{\kappa_T(0)}{2kT_0} x^2\right]^{-1 - \frac{\kappa}{\kappa_T(0)}} \quad (4.2)$$

This then gives us everything which is required to calculate the average rate of entropy production analytically with equation 3.57 and over many trajectories using equation 3.4. Figure 4.2 shows the results of these calculations over a range of  $\gamma$  (the code used to simulate the trajectories is included as an appendix) and it can be seen that the agreement improves as  $\gamma$  is increased. Despite this, it still seems to require us to go to much higher  $\gamma$  than would be expected (when compared with a similar approach in previous work where a different stationary profile was studied)[13] before the rates are in good agreement. This could well be the result of a problem which was only picked up much later on in the study, where for the stochastic calculations the initial positions and velocities were sampled from a Gaussian corresponding to isothermal Brownian motion (at  $T_0$ ) and it was assumed that they would quickly settle down into the correct distribution. Whilst this assumption appears to be fine for the velocity, it seems to be the case that it takes a much longer time than in the trajectories we have studied for the position distribution to change, especially when  $\gamma$  is large. This will be discussed in more detail in the next section. Figure 4.3 shows the total entropy production for  $\gamma = 60$  over a time interval of  $0 \rightarrow \frac{6\pi}{8}$ , which corresponds to three complete temperature cycles in the non-stationary case, when  $\omega = 8$ . Although there is still a slight deviation from the analytic result it was decided that this would be a sufficiently large value of  $\gamma$  to begin the study of the non-stationary temperature profile with.

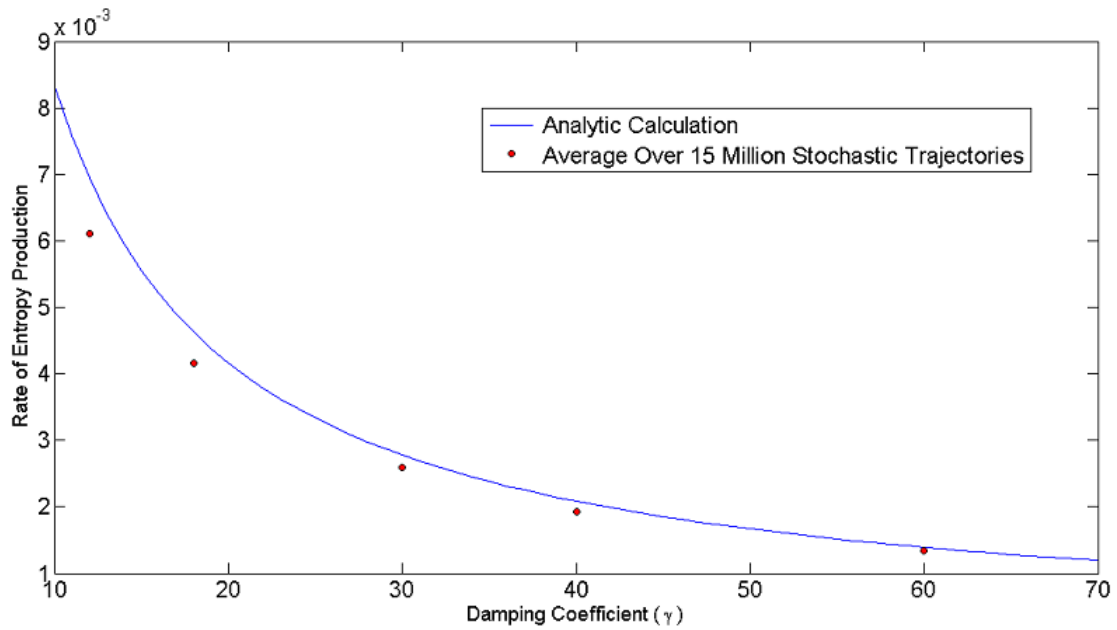


Figure 4.2: The rate of entropy production in the case of a stationary quadratic temperature profile as a function of  $\gamma$ . Stochastic average found over a time interval of  $t = \frac{6\pi}{8}$  using 20000 timesteps for each trajectory.

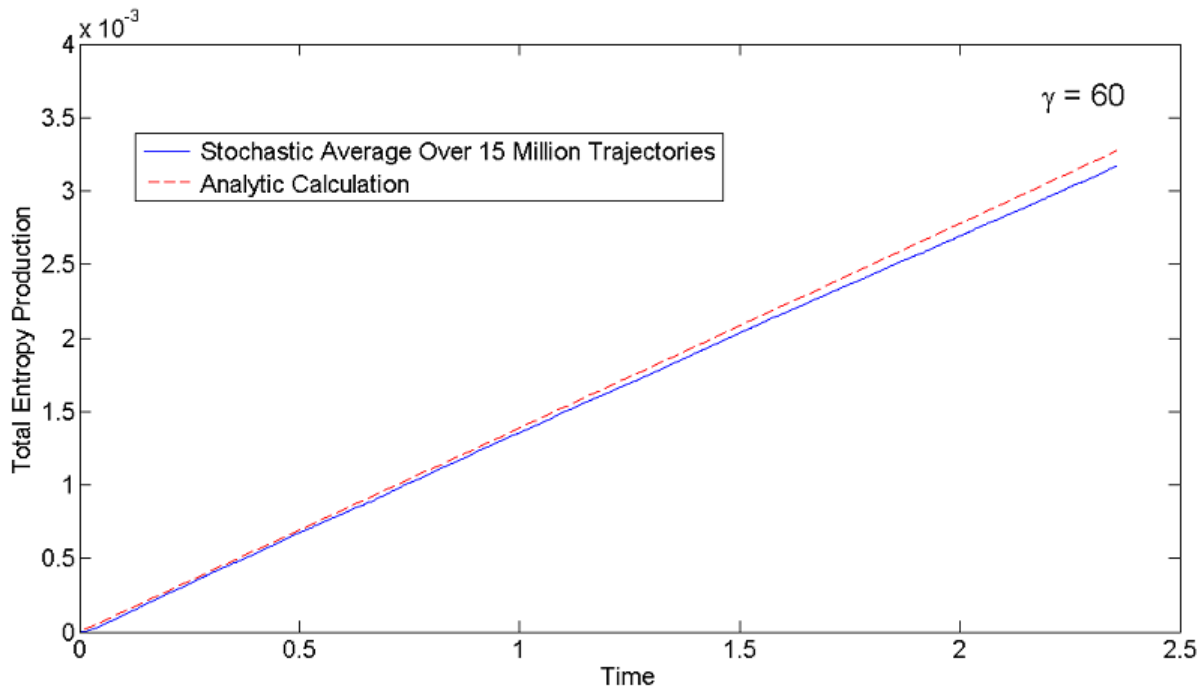


Figure 4.3: The total entropy production for the stationary profile in the case that  $\gamma = 60$  over a time interval of  $\frac{6\pi}{8}$  (which will correspond to three cycles in the non-stationary case).

## 4.2 Non-Stationary Temperature Profile

In this section the full temperature profile defined at the beginning of the chapter is implemented, however the approximation for  $\rho_{st}$  given in equation 4.2 is kept, where now  $T_r(x)$  should be interpreted as the time average of the reservoir temperature. This is because given that the approximation  $\bar{v} = 0$  is being employed it seems appropriate in light of equation 3.8 to use a time-independent  $\rho$ , but potential improvements to this model are discussed in section 4.3. Figure 4.4 shows a comparison of the analytically predicted entropy production obtained by integrating equation 3.57 over position and time with the average obtained by simulating 15 million particle trajectories. Again the initial  $x$  and  $v$  coordinates were chosen from a gaussian corresponding to a Brownian particle in equilibrium at  $T_0$ , and so the spike which is seen at the beginning of the average stochastic trajectory should be interpreted as the system settling down, however as mentioned in the previous section this will be a source of error as the position distribution takes a lot longer than the timescales studied here to relax properly. Despite this there is reasonably good agreement between the two curves, and it would appear that the PDF model being used is sufficient to capture at least all of the qualitative behaviour of the total entropy production. Figure 4.5 shows the contributions to the total entropy production from the system and medium entropy separately, averaged over the simulated particle trajectories. It is interesting to see that the system and medium components individually over a cycle are about an order of magnitude larger than the total entropy production, which suggests that the spatial transport of heat is low in comparison to the actual heat exchanges between the system and environment (as expected for large  $\gamma$ ). With hindsight it also looks like there may be a slight difference between the curves in the first cycle and the second cycle which again would suggest the system is still slowly relaxing, although it is not completely clear from this image and we would need to look at more temperature cycles to say for sure. Figure 4.6 then shows the distribution of total entropy production over the time interval  $\frac{2\pi}{\omega} \rightarrow \frac{6\pi}{\omega}$ , demonstrating that negative entropy values along a stochastic trajectory are not at all rare when studying small systems. It is also interesting to note how much larger quite typical values of  $\Delta S_{tot}$  can be when compared with the average.

It is of interest as well as being a good probe of how well the numerics of the system are working to look and see if the relevant fluctuation theorems are satisfied. For this system the integral fluctuation theorem should be satisfied for all times, and the detailed fluctuation theorem should hold over particular time intervals. The time intervals over which it should hold must be multiples of  $\frac{2\pi}{\omega}$  so that once the system is in a non equilibrium oscillatory state the probability density function is the same at the beginning and the end of the interval, and the driving protocol (the temperature of the heat bath in this case) must be symmetric about the midpoint. Results are shown in figure 4.7 (a) over the time interval  $t = \frac{7\pi}{2\omega} \rightarrow \frac{11\pi}{2\omega}$ , and despite the significant noise the overall trend seems reasonable except around the origin where there is a strange deviation. It is not really possible to attribute this to noise, especially given that it occurs in the region where the values of entropy production are most common and so it is a strong indication that something is not quite working as it should be.

Figure 4.7 (b) is a test of the integral fluctuation theorem over different lengths of time. Although the deviation from the expected result  $\langle \exp(-\Delta S_{tot}) \rangle = 1$  is small, the fact that it appears to increase when the time interval over which  $\Delta S_{tot}$  is sampled from is longer again indicates that there are some minor problems with the method being used. In particular it would seem to suggest that the probability density function being used is not an accurate enough representation of the underlying stochastic dynamics, which would either mean the model being used for the PDF is inadequate in some way or again that the system has not had sufficient time to settle down

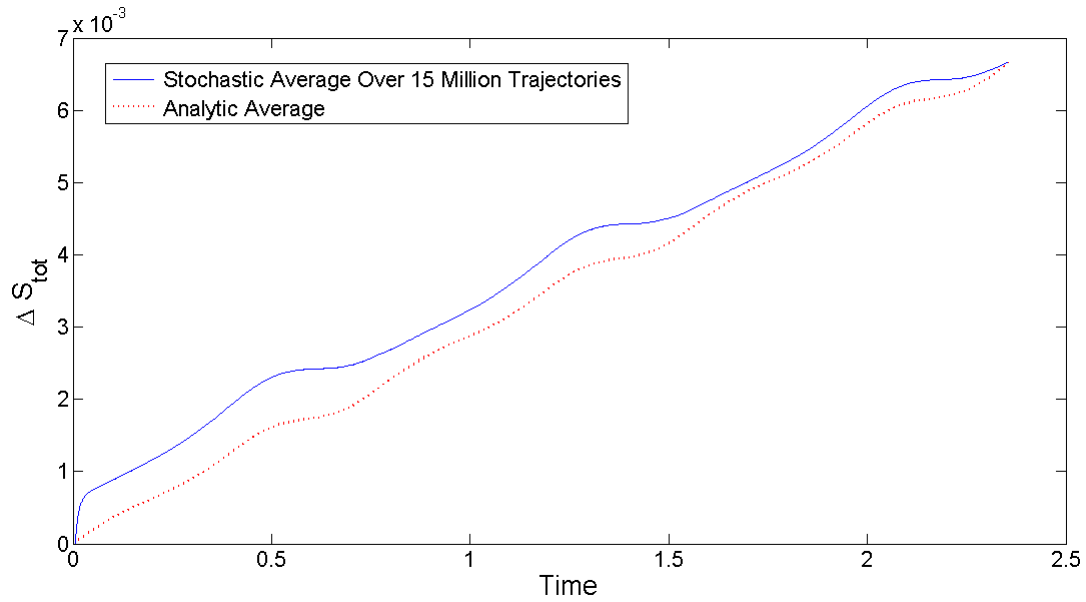


Figure 4.4: A comparison of the analytically predicted entropy production and the average entropy production over 15 million simulated trajectories. Each trajectory is composed of 20000 timesteps, representing an interval of  $\frac{6\pi}{\omega}$  (3 temperature cycles).

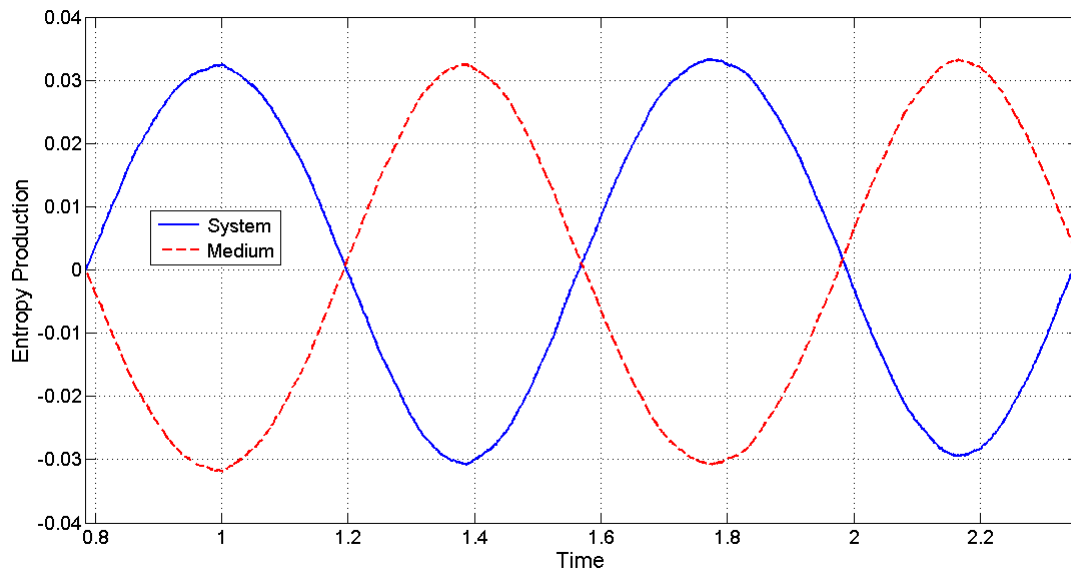


Figure 4.5: Comparison of the contribution to the total entropy production from the system and environment terms over two temperature cycles ( $t = \frac{2\pi}{\omega} \rightarrow \frac{6\pi}{\omega}$ ), averaged over 15 million trajectories.

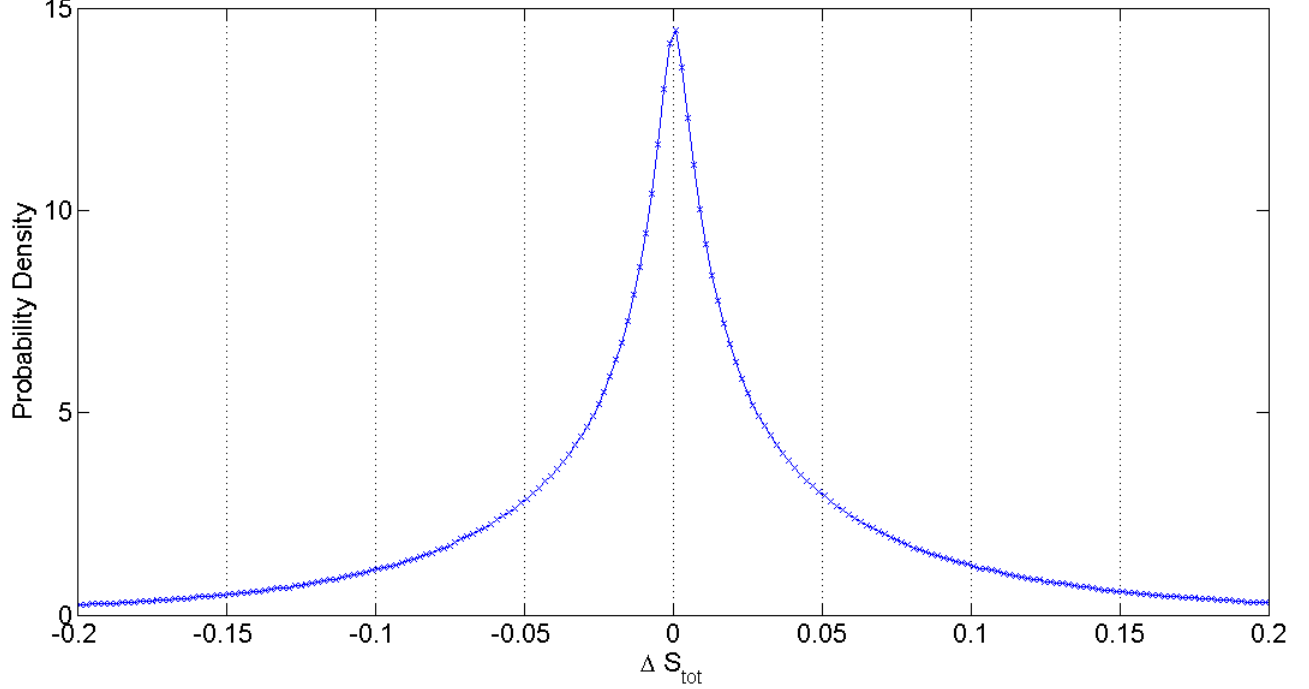


Figure 4.6: Distribution of the total entropy production over the time interval  $t = \frac{2\pi}{8} \rightarrow \frac{6\pi}{8}$  obtained from 15 million particle trajectories.

into the distribution predicted by the PDF.

The next thing which was tried was to calculate the average of the three components of the entropy production over many particle trajectories as well as looking at their distributions. Analytically the averages can be calculated from the equations in section 3.4, and the increments along any stochastic trajectory are given by[13]:

$$d\Delta S_1 = -d(\ln(p)) - \frac{\partial\beta}{\partial x}dx - \frac{\partial\beta}{\partial v}dv - \frac{kT_r\gamma}{m} \frac{\partial^2\beta}{\partial v^2} \quad (4.3)$$

$$d\Delta S_2 = \frac{-v\kappa x}{kT_r}dt - \frac{vm}{kT_r}dv + \frac{\partial\beta(\hat{T}\mathbf{x})}{\partial x}dx - \frac{\partial\beta(\hat{T}\mathbf{x})}{\partial(-v)}dv + \frac{kT_r\gamma}{m} \left[ \frac{\partial\beta(\hat{T}\mathbf{x})}{\partial(-v)} \right]^2 dt - v \frac{\partial\beta(\hat{T}\mathbf{x})}{\partial x}dt - \left(-\gamma v + \frac{\kappa x}{m}\right) \frac{\partial\beta(\hat{T}\mathbf{x})}{\partial(-v)}dt \quad (4.4)$$

$$d\Delta S_3 = \ln \left( \frac{p_{st}(\mathbf{x})p_{st}(\hat{T}\mathbf{x}')}{p_{st}(\mathbf{x}')p_{st}(\hat{T}\mathbf{x})} \right) \quad (4.5)$$

where  $\beta(\mathbf{x}) = -\ln(p_{st}(\mathbf{x}))$  and the  $\mathbf{x}'$  means evaluation at the end of the incremental timestep as opposed to the beginning. These quantities were then all calculated over particle trajectories of the same length as before and with the same number of timesteps, with the results being shown in figures 4.8, 4.9 and 4.10.

The most interesting of these is probably  $\Delta S_1$  shown figure 4.8, where it can be seen that although the overall gradient is similar there is quite a significant difference between the analytically predicted average and the average over particle trajectories, especially in the first half of each temperature cycle when the system is being heated. As well as some potential problems already mentioned, it could also be the case that the value of

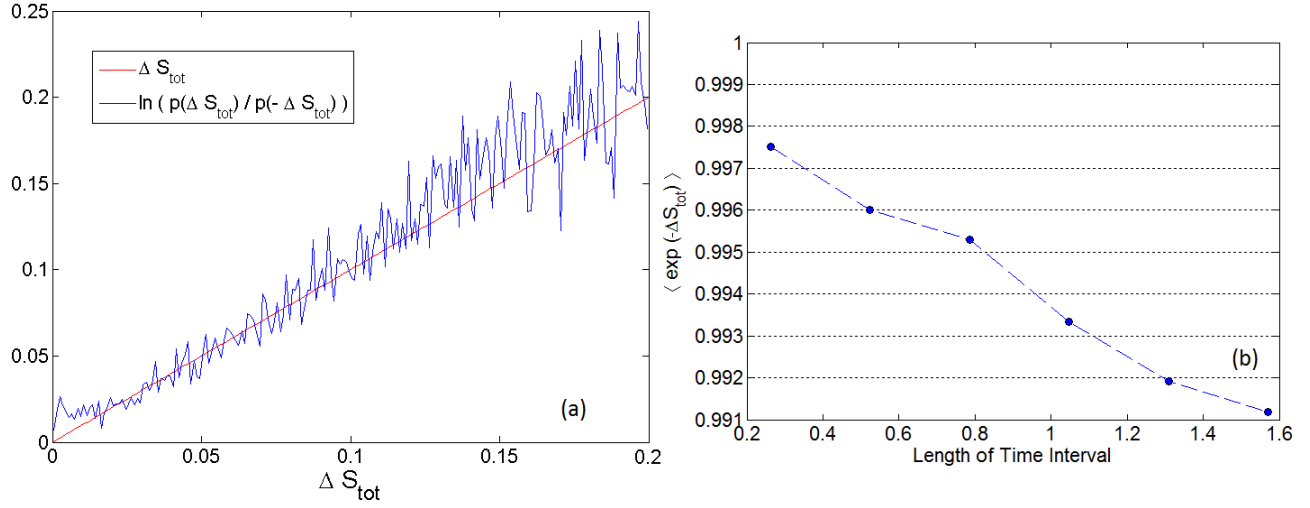


Figure 4.7: (a) Test of detailed fluctuation theorem over the interval  $t = \frac{7\pi}{2\omega} \rightarrow \frac{11\pi}{2\omega}$ . Results obtained from simulation of 15 million particle trajectories and collecting the data into 400 bins for values of  $\Delta S$  between  $\pm 0.2$ . (b) Test of integral fluctuation theorem over different lengths of time (between  $t = \frac{2\pi}{\omega} \rightarrow \frac{6\pi}{\omega}$ ).

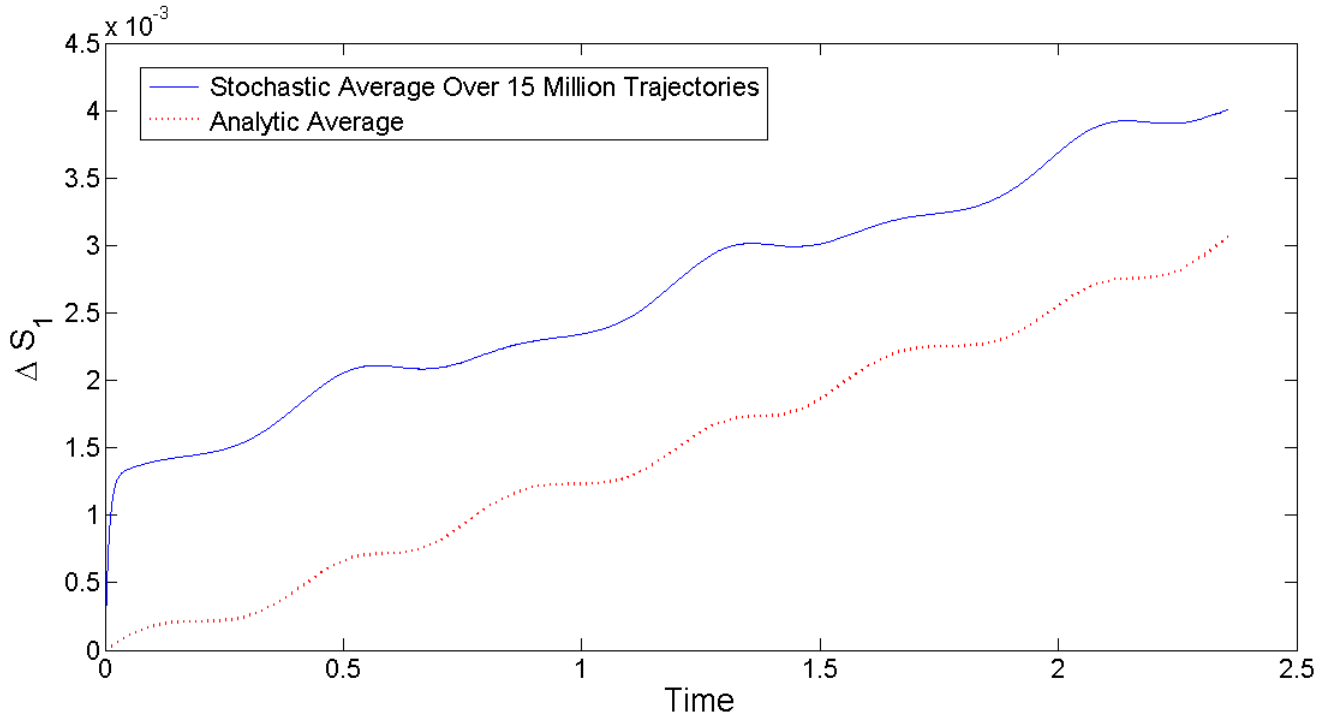


Figure 4.8: Comparison of the average of  $\Delta S_1$  predicted analytically and calculated from the simulation of 15 million particle trajectories. Trajectories are over a time interval of three temperature cycles and composed of 20000 timesteps each. Initial  $x$  and  $v$  coordinates are chosen from a Boltzmann distribution at  $T_0$ .

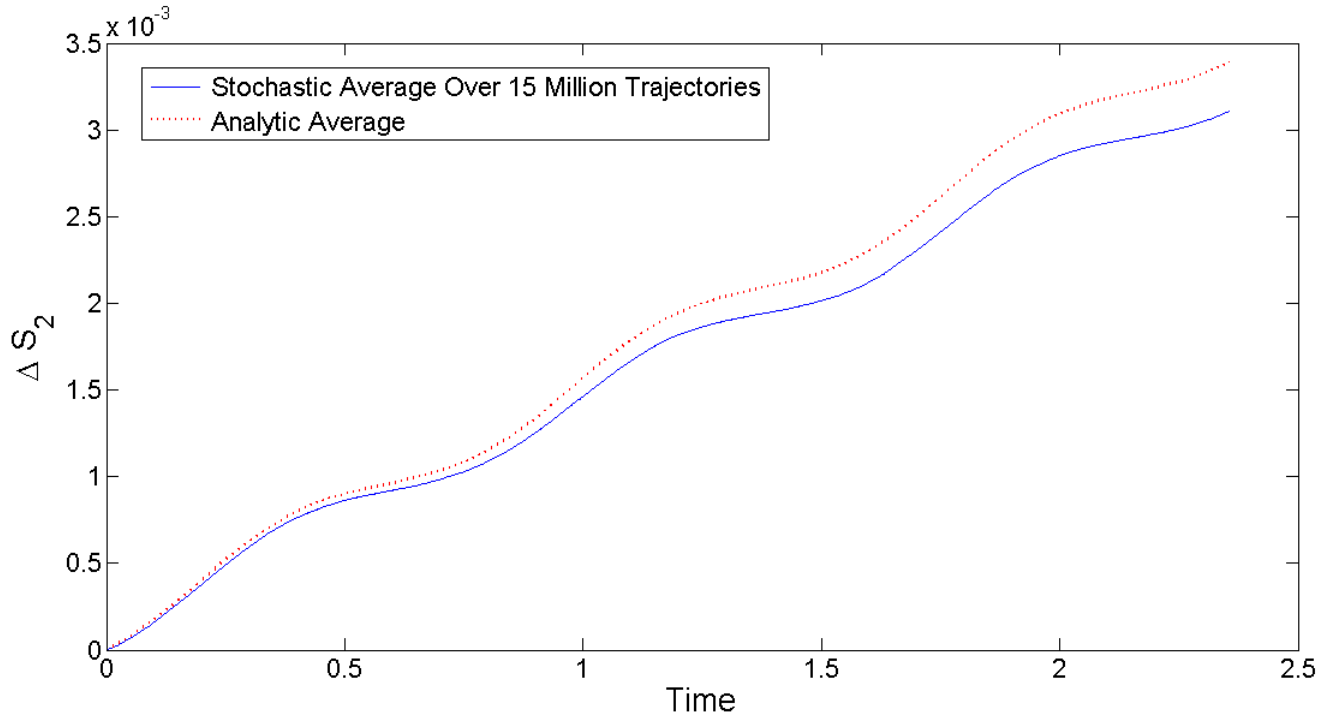


Figure 4.9: Comparison of the average of  $\Delta S_2$  predicted analytically and calculated from the simulation of 15 million particle trajectories. Trajectories are over a time interval of three temperature cycles and composed of 20000 timesteps each. Initial  $x$  and  $v$  coordinates are chosen from a Boltzmann distribution at  $T_0$ .

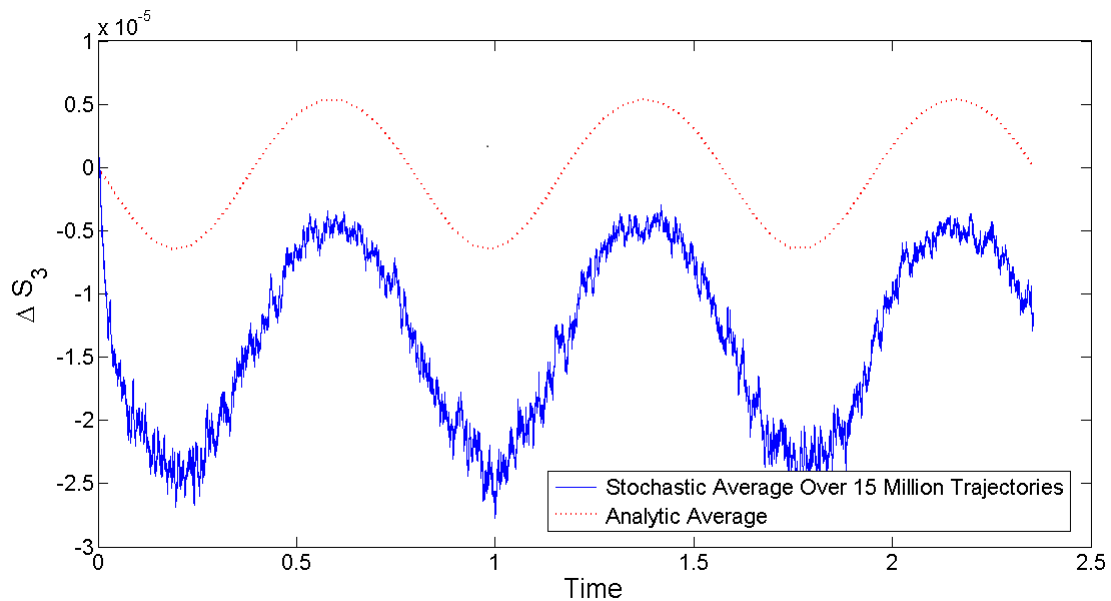


Figure 4.10: Comparison of the average of  $\Delta S_3$  predicted analytically (using the full expression in equation 3.60 rather than just to first order in  $\frac{1}{\gamma}$ ) and as calculated from the simulation of 15 million particle trajectories. Trajectories are over a time interval of three temperature cycles and composed of 20000 timesteps each. Initial  $x$  and  $v$  coordinates are chosen from a Boltzmann distribution at  $T_0$ .

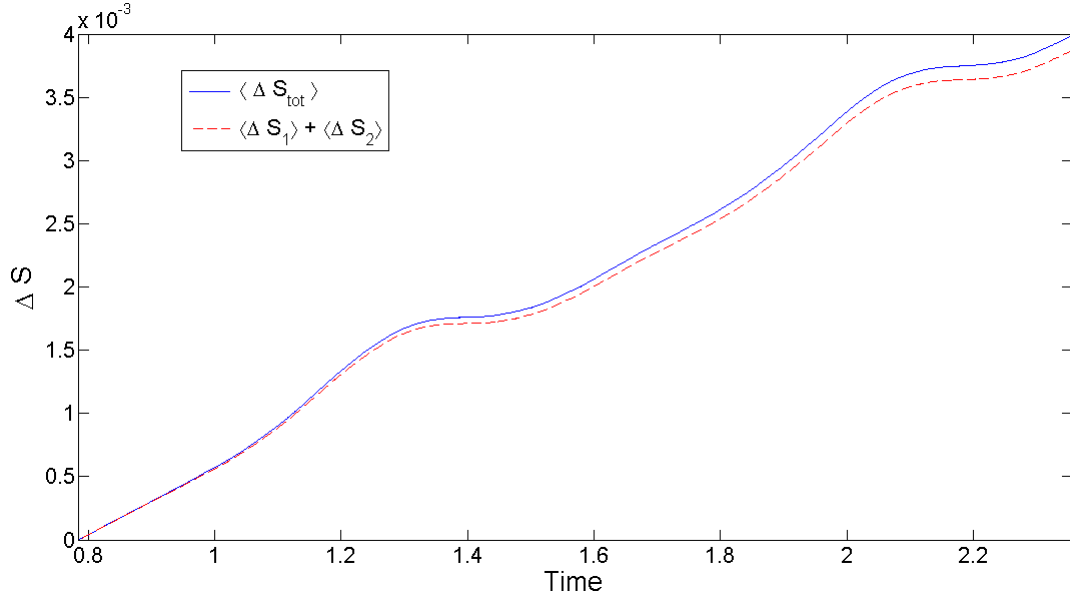


Figure 4.11: Comparison of the average of  $\Delta S_{tot}$  calculated as in figure 4.4 and by adding the average of  $\Delta S_1$  and  $\Delta S_2$  over 15 million particle trajectories between  $t = \frac{2\pi}{8} \rightarrow \frac{6\pi}{8}$

the parameter  $B$  being used it too large, so that the rate of change in the temperature profile is too large to justify the use of the approximation  $\bar{v} = 0$ . There also appear to be regions of slightly negative production, which is in violation of the integral fluctuation theorem; another problem which needs to be explained. The agreement between the two plots shown in figure 4.9 for  $\Delta S_2$  is qualitatively a lot better than with  $\Delta S_1$ . As  $S_2$  is associated with the imposition of a non-equilibrium constraint and  $S_1$  with the relaxation towards a stationary state, the inclusion of  $\bar{v} \neq 0$  into the model would not affect  $\Delta S_2$  which perhaps would support the idea that the qualitative difference in the analytic and stochastic  $\Delta S_1$  is a result of the approximation  $\bar{v} = 0$ .

Although we showed that to first order in  $\frac{1}{\gamma}$  that  $\langle \Delta S_3 \rangle = 0$  it is still possible to calculate an analytic average by using the full expression in equation 3.60 as well as calculating an average over the particle trajectories and this is shown in figure 4.10. It is worth pointing out that really with the approximations employed any calculation involving quantities of order  $\frac{1}{\gamma^2}$  or higher cannot really be trusted to be reliable, however the qualitative agreement between the two is reasonable and we see that as expected  $\Delta S_3$  is not always positive on average. The average calculated over particle trajectories is very noisy, but this is not necessarily surprising when it is realized that the distribution of  $\Delta S_3$  covers a range of values many orders of magnitude larger than the average and as such it is a very small signal being picked out.

Figure 4.11 shows the average total entropy averaged from the particle trajectories shown in fig. 4.4 compared to the sum of the average of  $\Delta S_1$  and  $\Delta S_2$ . Although they are almost the same, the fact that they differ at all is strange and difficult to explain as ultimately they should be the average of the same quantities (albeit expressed in different ways, and ignoring  $\Delta S_3$  which is entirely negligible). Whether this is due to an error in the code being used or something else has not yet been determined.

The distributions for each of the components is shown in figure 4.12 and compared to the distribution of the total entropy. Clearly  $\Delta S_3$  has a much narrower peak than the other components, but they all take on

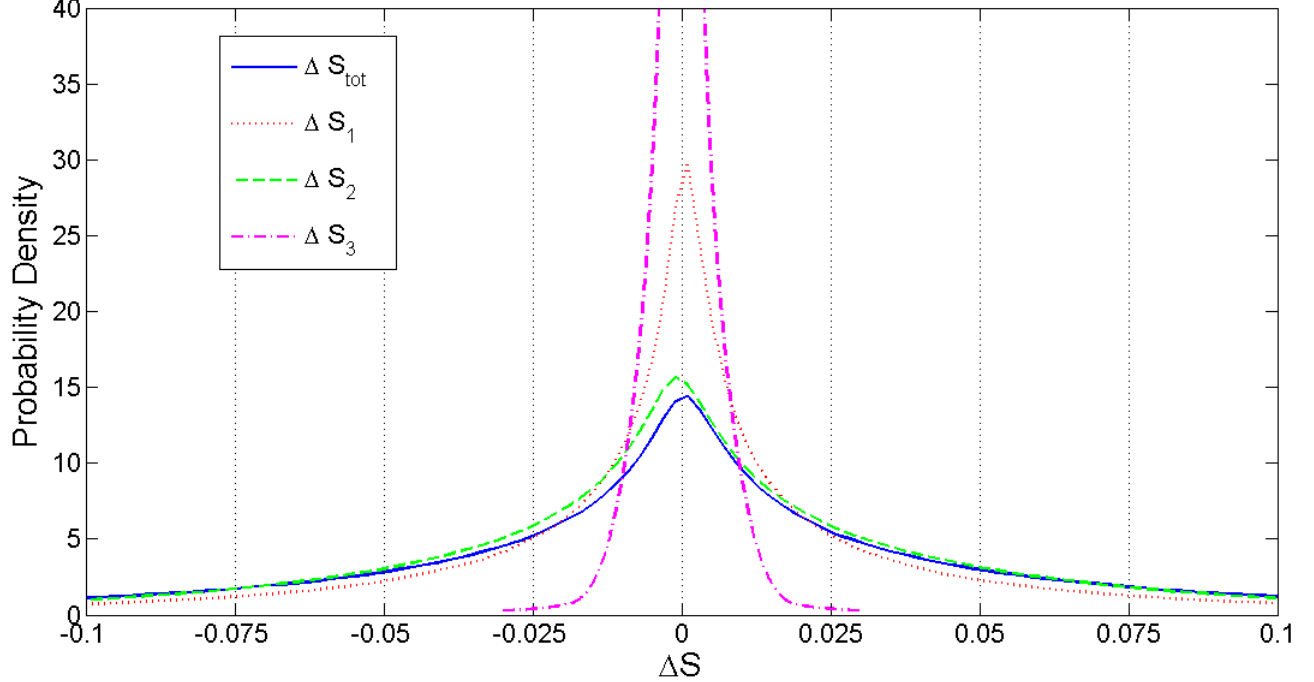


Figure 4.12: Distributions of  $\Delta S_{tot}$ ,  $\Delta S_1$ ,  $\Delta S_2$  and  $\Delta S_3$  from  $t = \frac{2\pi}{8} \rightarrow \frac{6\pi}{8}$ .

a wide range of values when compared to their averages. It is strange to see that the peak of  $\Delta S_2$  is shifted slightly to the left of the origin, so that despite there being a positive average in total the most probable value is actually negative; very much an unexpected result. Figure 4.13 shows a comparison of the distribution of position values at different times over one temperature cycle compared to the model of  $\rho_{st}$  being used, and figure 4.14 shows the same for the velocity, compared to  $\int p dx$  at different times. It can be seen that there is a slight variation in the velocity distribution over the temperature cycle which is well predicted by the probability distribution function being employed (in figure 4.14 the circles represent  $\int p dx$  where the corresponding line is the distribution obtained from binning velocity values along the particle trajectories), but there is no detectable variation in the position distribution. This does provide evidence that a stationary  $\rho$  should be a good approximation, however the position distribution does not actually match up with  $\rho_{st}$  very well. The reason for this is as alluded to earlier that the initial position values were sampled from a normal distribution and there has not been enough time to relax into the correct distribution, which can be demonstrated by running the stochastic equations of motion for a much longer period of time and seeing that eventually the position distribution does change. This is shown in figure 4.15 for a time of  $\Delta t = 50$ , at which point  $\rho_{st}$  is then a very good approximation of the distribution. Unfortunately as this was only spotted late on in the project the effect this has on all of the previous results has not yet been fully investigated, but it does not fully account for the deviation in  $\Delta S_{tot}$  away from what is predicted analytically. This is demonstrated in figure 4.16 which shows a comparison of the previous total entropy production from figure 4.4 compared with the average total entropy production when the initial positions for the particle trajectories are sampled from the corrected distribution shown in figure 4.13, over the time interval  $t = \frac{2\pi}{8} \rightarrow \frac{6\pi}{8}$ . There is a distinct difference between the two and it's debatable as to whether the agreement with the analytically predicted curve is improved or not. On one hand the total entropy produced over one temperature cycle is a lot closer to what is expected, however during the actual cycle the curves seem to deviate more. This becomes even stranger when looking at what happens

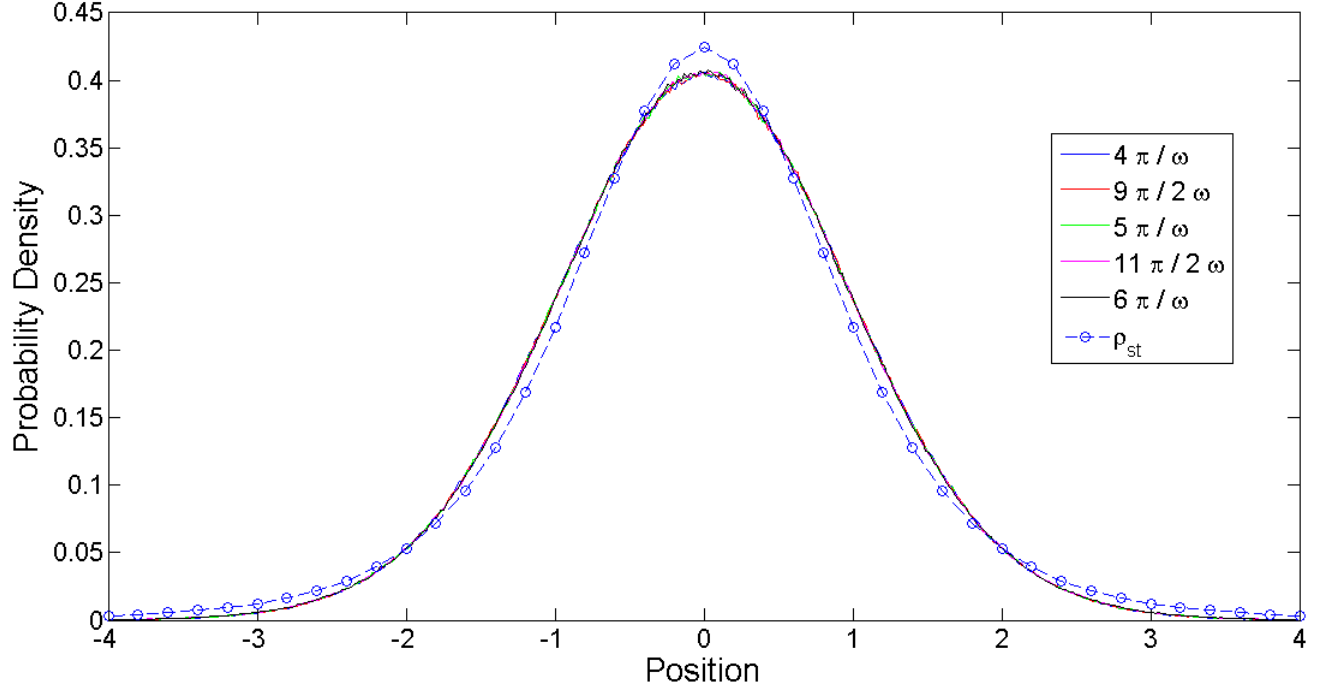


Figure 4.13: Distribution of positions over one temperature cycle from  $t = \frac{4\pi}{\omega} \rightarrow \frac{6\pi}{\omega}$  compared with the stationary approximation being used for  $\int p \, dv \approx \rho_{st}$ . Positions are sampled from 15 million trajectories

to  $\Delta S_1$  which is shown in figure 4.17. Now despite the end point of each cycle again agreeing reasonably well with the analytic value, during the cycle the curves are very different and the problem of negative production over certain time intervals seems to be even worse. Clearly there is another problem here which needs further investigation. Figure 4.18 shows a comparison with  $\Delta S_2$  and we see that there is negligible when the initial position distribution is corrected. It would be interesting to see how these new results affect the adherence of  $\Delta S_{tot}$  to both the integral fluctuation theorem and detailed fluctuation theorem, as perhaps this would give a better idea as to whether these latest results are actually better or worse than before. Something else which was not done was to check whether  $\Delta S_1$  and  $\Delta S_2$  obey the integral fluctuation theorem, but looking at figure 4.17 this seems unlikely for the latest results with  $\Delta S_1$ . It may also be the case that  $\Delta S_1$  and  $\Delta S_2$  are supposed to obey the detailed fluctuation theorem over the same interval as  $\Delta S_{tot}$ , which would have been interesting to check.

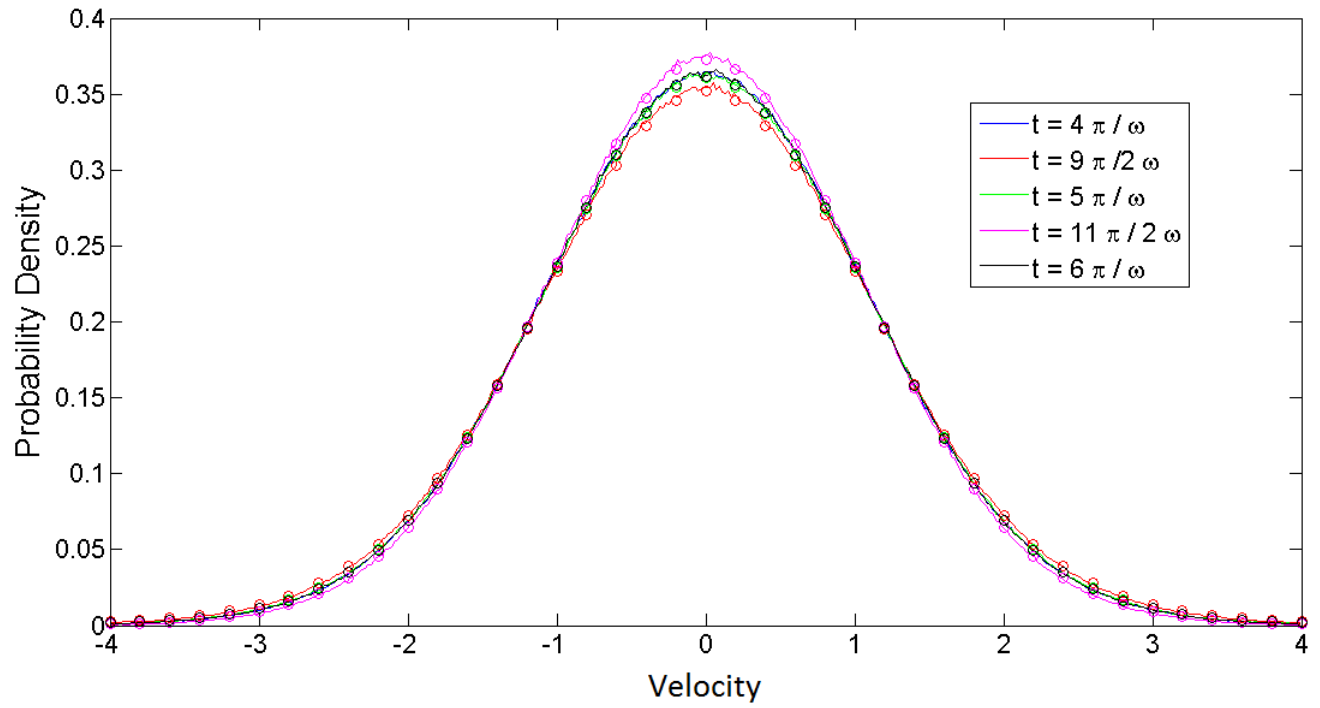


Figure 4.14: Distribution of velocities over one temperature cycle from  $t = \frac{4\pi}{\omega} \rightarrow \frac{6\pi}{\omega}$  compared with  $\int p dx$  (circles) at different times. Velocities are sampled from 15 million trajectories.

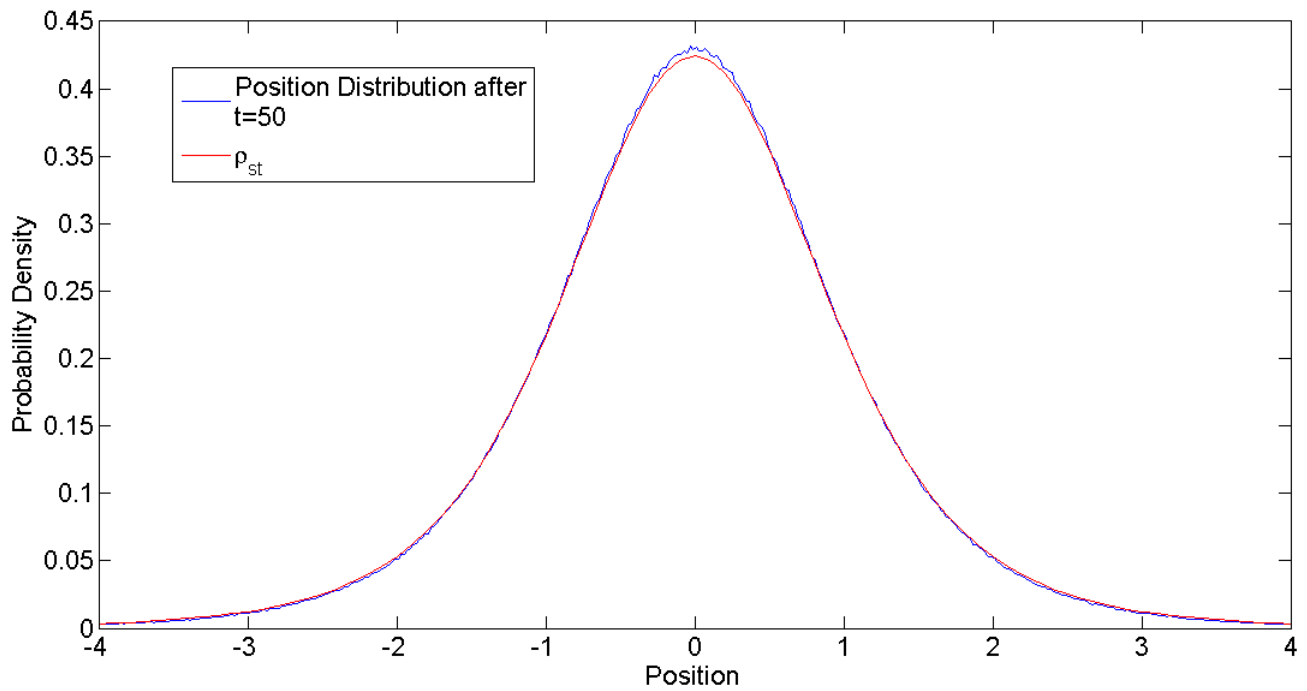


Figure 4.15: Distribution of initial positions after a long period ( $t = 50$ ) of running the stochastic evolution from an initial isothermal Gaussian distribution, compared with  $\rho_{st}$ .

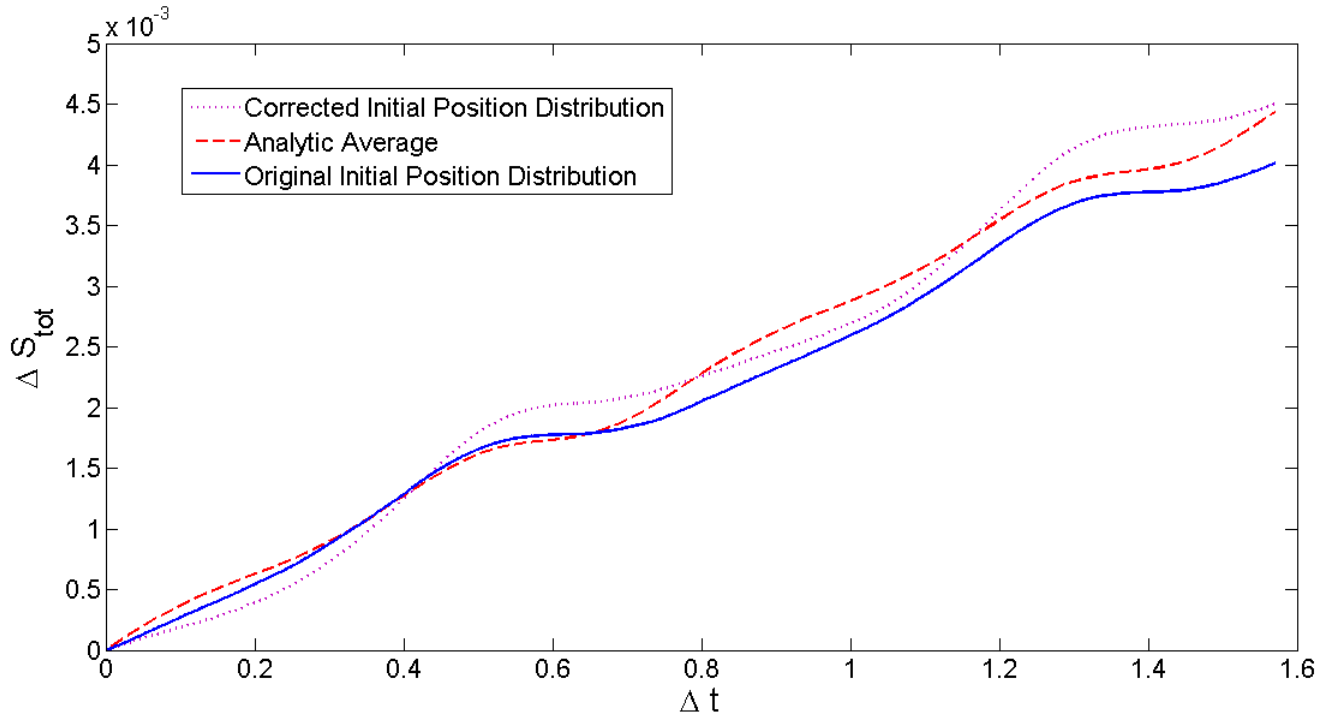


Figure 4.16: Demonstration of how using the corrected initial position distribution changes the average total entropy production obtained from the simulation of particle trajectories. Plot shows entropy production only over the interval  $t = \frac{2\pi}{8} \rightarrow \frac{6\pi}{8}$  (two temperature cycles)

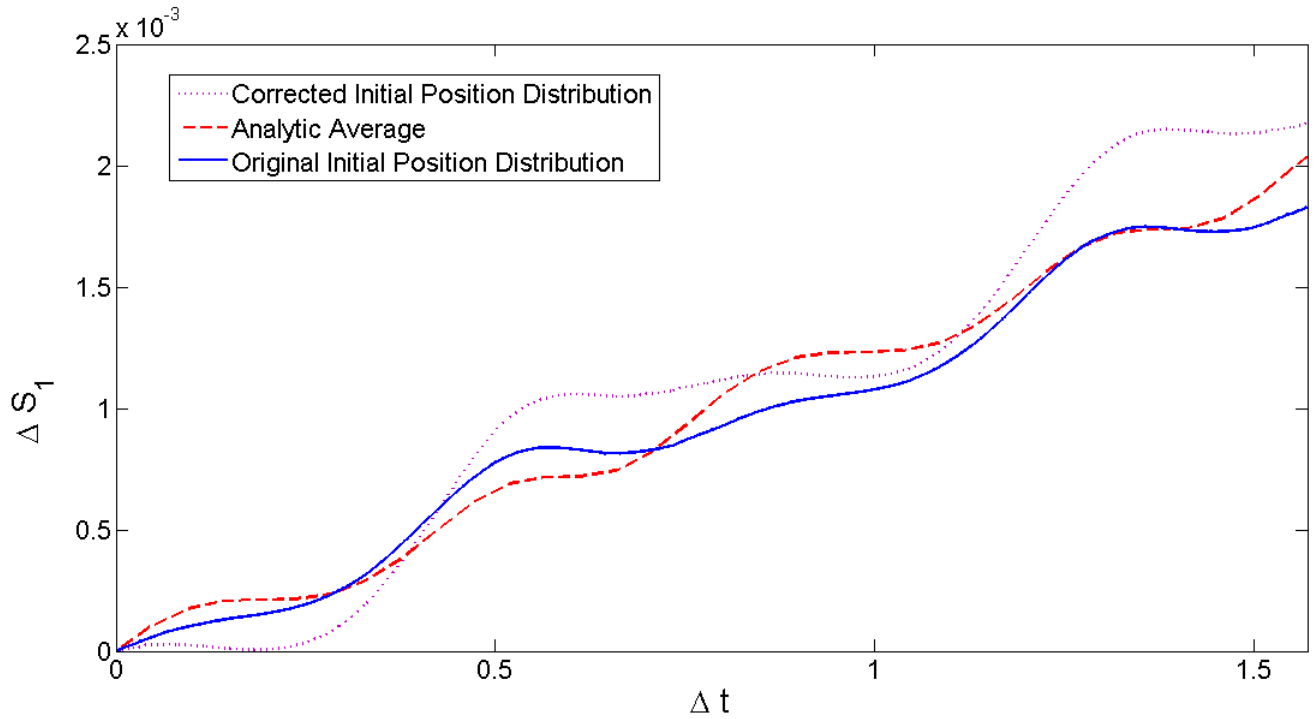


Figure 4.17: Demonstration of how using the corrected initial position distribution changes the average production of  $\Delta S_1$  obtained from the simulation of particle trajectories. Plot shows entropy production only over the interval  $t = \frac{2\pi}{8} \rightarrow \frac{6\pi}{8}$  (two temperature cycles)

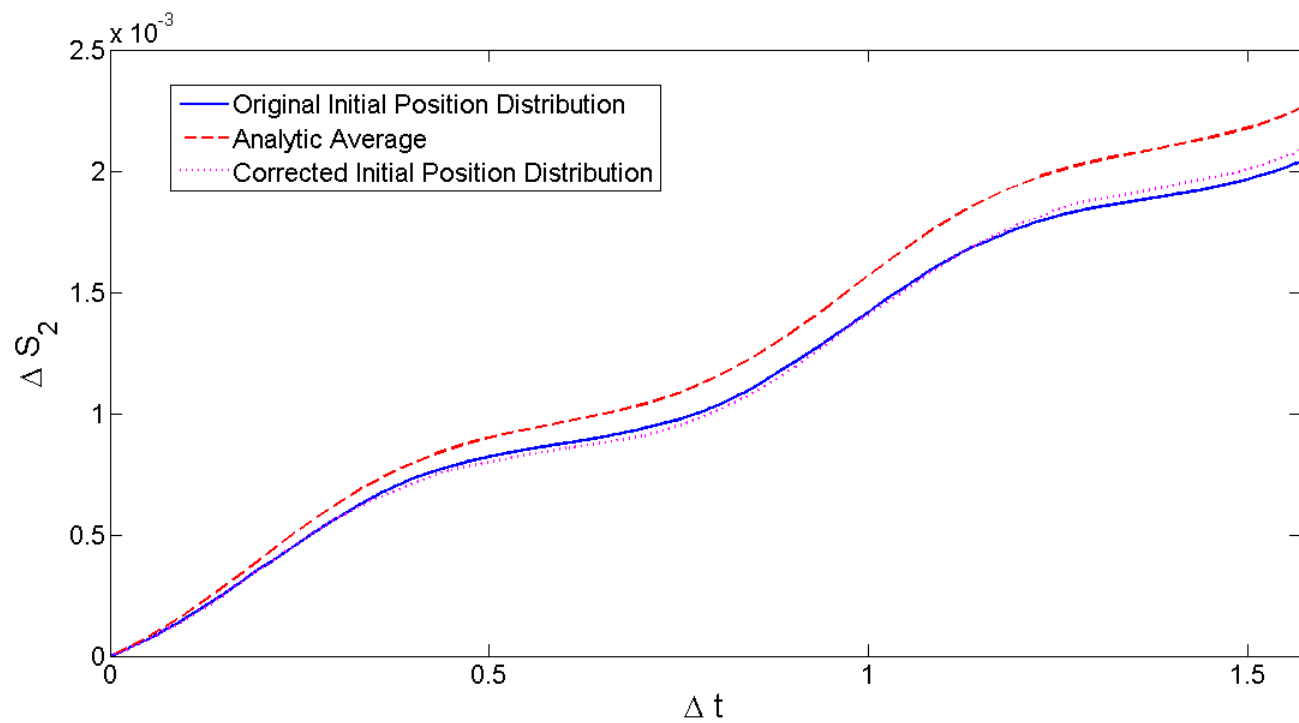


Figure 4.18: Demonstration of how using the corrected initial position distribution changes the average production of  $\Delta S_2$  obtained from the simulation of particle trajectories. Plot shows entropy production only over the interval  $t = \frac{2\pi}{8} \rightarrow \frac{6\pi}{8}$  (two temperature cycles)

### 4.3 Improving the model for $\rho$

Although figures 4.13 and 4.15 suggest that a stationary approximation for  $\rho$  should be reasonable, it is nevertheless still a limitation of the model being employed. One way to go about improving it is to use equations 3.8 and 3.9, which along with the evaluation of  $\bar{v}^2$  found in equation 3.50 give two differential equations in terms of  $\rho$  and  $\bar{v}$ . Solving these equations has been attempted in Mathematica, however it is not entirely obvious what the appropriate boundary conditions to impose are. The conditions which have been tried are  $\rho(x, 0) = \rho_{st}$ ,  $\bar{v}(x, 0) = 0$  and then assuming that  $\rho$  and  $\bar{v}$  go to zero at the boundary, and the result is shown in figure 4.17. Clearly the condition that  $\bar{v} \rightarrow 0$  at the boundaries is not correct and has been ignored by Mathematica. The results seem physically reasonable;  $\bar{v}$  is an odd function of position and varies periodically, as well as increasing in magnitude for larger  $x$  where the variation in temperature is also largest. There are only very slight variations in  $\rho$  from  $\rho_{st}$  which can be seen more clearly in figure 4.18 where  $\rho$  is plotted for particular values of  $x$ . The variation in time would be expected to be periodic, and we see this is almost the case however the values are falling slightly after each period. This is not a result of the system settling down as it appears to occur for all values of  $x$ , and so there is a clear problem with this solution in that probability seems to be leaking away. It is also the case that trying to solve the equations over a longer period of time or over too wide a range of position values causes the solution to break down, which is another reason to doubt its reliability. Nevertheless it is of interest to see whether using this model has any effect on the entropy production. Figure 4.19 (a) shows the difference between the average total entropy production calculated over many particle trajectories between this and the  $\rho = \rho_{st}, \bar{v} = 0$  model (note this was done using the uncorrected initial position distribution), and (b) shows the analytic difference (for this new model the average is calculated numerically directly from equation 3.16). In both cases the difference is very small, which if the solutions found for  $\rho$  and  $\bar{v}$  found can in anyway be trusted would suggest that the  $\rho = \rho_{st}, \bar{v} = 0$  approximation is good enough for the parameters being used, meaning that the problems with previous results are still without explanation. Something which could be interesting would be to try and calculate an approximate  $\rho$  and  $\bar{v}$  in a slightly different way and compare with the method used here. Perhaps a reasonable approximation for  $\rho$  would be given by  $\rho \approx \frac{1}{T(x,t)} \exp\left(\int_0^x dx' \frac{-\kappa x'}{kT(x',t)}\right)$  with  $T(x,t) = T_r(x,t) - \frac{1}{2\gamma} \frac{\partial T_r}{\partial t}$  as in equation 3.54.  $\bar{v}$  could then be calculated from the continuity equation (equation 3.8), although again there may be a problem with what boundary conditions to impose. If we could assume  $\rho \bar{v} \rightarrow 0$  as  $|x| \rightarrow \infty$  then we can write

$$\rho(x,t)v(\bar{x},t) = \int_{-\infty}^x \frac{\partial \rho}{\partial t} dx' \quad (4.6)$$

however it is not necessarily obvious whether this would be a valid thing to do. Unfortunately there has not been enough time to investigate this more carefully.

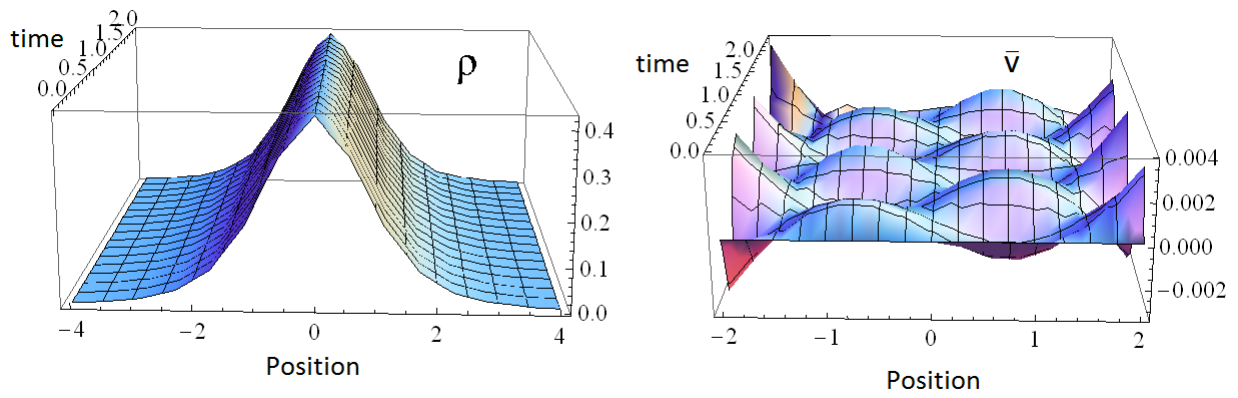


Figure 4.19:  $\rho$  and  $\bar{v}$  calculated numerically from equations 3.8 and 3.9 in Mathematica.

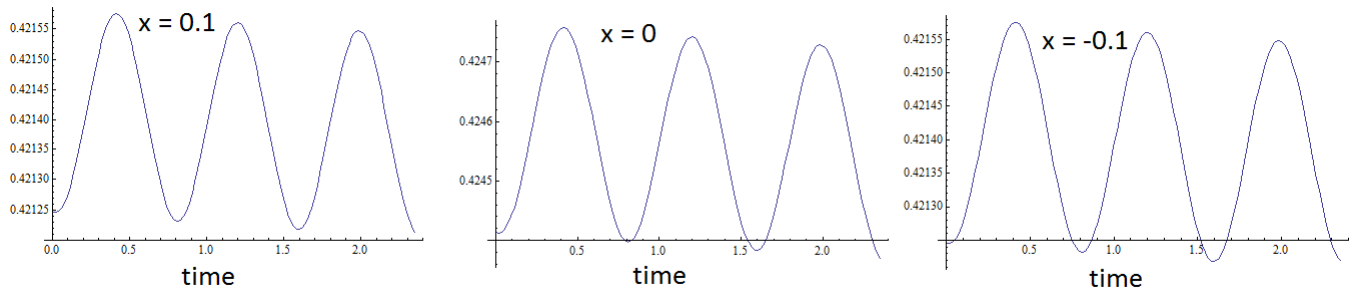


Figure 4.20:  $\rho$  as calculated for figure 4.17, but taken at specific values of  $x$  over the three temperature cycles.

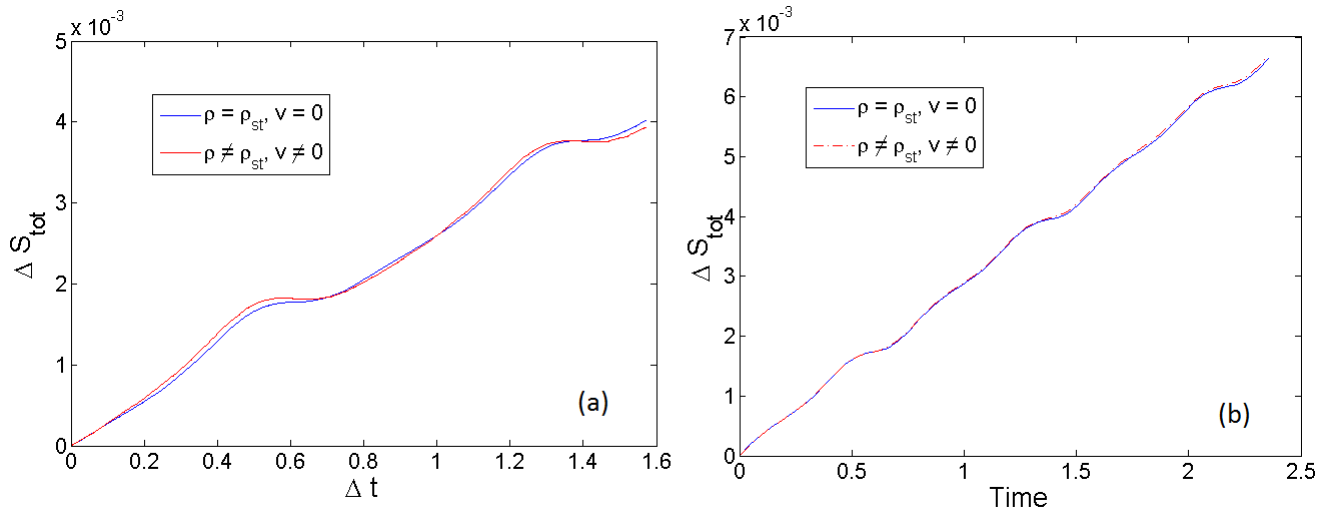


Figure 4.21: (a) Average total entropy production obtained with this newer model compared to the previous result, calculated by simulation of particle trajectories. (from  $t = \frac{2\pi}{\omega} \rightarrow \frac{6\pi}{\omega}$  (here still using the incorrect initial position distribution)) (b) Average total entropy production predicted analytically for both models. ( $t = 0 \rightarrow \frac{6\pi}{\omega}$ )

## Chapter 5

# Conclusion

Overall the aims of the project have been achieved to a limited degree. There seem to be promising signs that the method being employed is close to working properly and analytic and numerically simulated averages for the total entropy and its three components have been calculated and are reasonably close to agreement. However certainly there are problems which still need to be addressed, as something is not quite working as it should be. Potential problems have been discussed and include some of the approximations used in solving the Kramers equation as well as perhaps needing to think about using parameters corresponding to a slower change in the heat bath temperature profile. However as the latest results were obtained too recently for them to be thoroughly investigated, it seems likely there may be another unaccounted for source of error as well.

# Appendix A

## Code to Simulate Particle Trajectories

This is the C++ code used for the simulation of particle trajectories. Note that  $\Delta S_1$  is calculated using Stratonovich rules[11], rather than Ito calculus introduced in chapter 2. This was done as the expression is a little simpler using these rules, although in retrospect this slight simplification is not really worth it for how much more unpleasant it makes the code to read by having to define a number of additional variables. Also in retrospect another obvious simplification would have been to define a function for  $p_{st}$  rather than defining so many variations as separate arrays. In its current form it is designed to run on the UCL legion cluster.

```
1 #define _USE_MATH_DEFINES
3 #include <iostream>
  #include <math.h>
5 #include <time.h>
  #include <cstdlib>
7 #include <random>
  #include <fstream>
9 #include <sstream>

11 using namespace std;

13 int main(int argc, char *argv[]) {
15     int jobno = atoi(argv[1]); // take job number from legion, so that the random seed is different for
      each run.

17     srand(time(NULL)+jobno); // seed RNG

19     int k = 1000000; // number of trajectories
      int N = 20000; // number of timesteps per trajectory

21     // define important constants

23     double w = 8.0; // angular frequency
25     double T = 6*M_PI/w; // period of trajectory (3 cycles)
      double dt = T/(N-1); // time increment
27     double sqdt = sqrt(dt); // square root of dt
      double kappa = 1; // force constant of confining potential
29     double m = 1; // particle mass
      double gamma = 60.0; // damping coefficient
31     double boltzmannk = 1.0; //using units of k=1
      double T0 = 1.0; // temp at origin (at t=0)
33     double B = 0.2; // coefficient for t-dependence of reservoir temp
      double A = 0.5; // coefficient for spatial dependence of reservoir temp
35     double dx = 0.00001; /* used for evaluating derivatives. Small enough for expressions to agree with
```

```

evaluation of full expression in Mathematica to at least 5 s.f.*/
37
//initialize RNG for normal distribution
39 default_random_engine generator;
generator.seed(time(NULL)+jobno);
41 normal_distribution<double> distribution(0.0,1.0); //distribution has mean 0, stddev 1

43
//declare array variables:
45 double *av_traj, *av_traj_sys, *av_traj_med, *av_traj_ds1, *av_traj_ds2, *av_traj_ds3, *dSsys,
*dSmed, *dS1, *dS2, *dS3, *Straj, *Straj1, *Straj2, *Straj3, *Smedtraj, *Ssystraj,
47 *STOT, *S1TOT, *S2TOT, *S3TOT, *x, *v, *str_x, *str_v, *dW, *temp, *dtemp, *str_temp,
*str_dtemp, *dtemp, *str_tempplus, *str_tempminus, *str_dtempplus, *str_dtempminus,
49 *tempplus, *tempminus, *dtempplus, *dtempminus, *pdf, *pstat, *str_pstatp,
*str_pstatmx, *str_pstatpv, *str_pstatmv, *pstatp, *pstatpx, *pstatmx, *pstatpv, *pstatmv;
51

53 av_traj = new double[N]; // av. stot at each timestep
av_traj_sys = new double[N]; // av. s_sys at each timestep
55 av_traj_med = new double[N]; //av. s_med at each timestep
av_traj_ds1 = new double[N]; // '' s_1 ''
57 av_traj_ds2 = new double[N]; // '' s_2 ''
av_traj_ds3 = new double[N]; // '' s_3 ''
59

//variables for storing the final value of entropy for each trajectory.
61 STOT = new double[k];
S1TOT = new double[k];
63 S2TOT = new double[k];
S3TOT = new double[k];
65

67 for(int y=0; y<N; y++) {
av_traj[y]=0.0;
69 av_traj_sys[y]=0.0;
av_traj_med[y]=0.0;
71 av_traj_ds1[y]=0.0;
av_traj_ds2[y]=0.0;
73 av_traj_ds3[y]=0.0;
}
75

77 //start iteration of k trajectories
for(int i=0; i < k; i++) {
79
//generate random noise for each timestep of the trajectory
81 dW = new double[N];

83 for(int r=0; r < N; r++) {
dW[r] = distribution(generator) * sqdt;
85 }

87
/*Note on variables which begin with str_....
89 Used to evaluate Delta S_1 as the expression using Stratonovich calculus is simpler (
alternative to Ito calculus,
see reference X), but the expressions must be evaluated at the midpoint of each incremental
timestep. In hindsight
91 this wasn't necessary. */

93 //declare variables to be used for each trajectory.
v = new double[N]; // velocity along trajectory
95 x = new double[N]; //position along trajectory
str_v = new double[N]; // velocity at the midpoint of each timestep i.e. 0.5(v[j+1]+v[j])
97 str_x = new double[N]; // position at midpoint of each timestep
temp = new double[N]; // temperature at point on trajectory.
99 tempplus = new double[N]; //evaluated at x[j]+dx (to evaluate derivatives)

```

```

tempminus = new double[N]; // evaluated at x[j]-dx
101 str_temp = new double[N]; // temp with position evaluated at midpoint of timestep.
str_tempplus = new double[N]; /*temp evaluated at slightly larger x value. Used for
103     derivative of pstat*/
str_tempminus = new double[N]; // temp at slightly lower x value
105 dtempx = new double[N]; // derivative of temp wrt x at each point on trajectory
dtempxplus = new double[N];
107 dtempxminus = new double[N];
str_dtempx = new double[N]; // as above evaluated at midpoint.
109 str_dtempxplus = new double[N]; //deriv of temp wrt x evaluated at slightly larger x
str_dtempxminus = new double[N]; // eval. slightly lower x.
111 dtempt = new double[N]; // derivative of temp wrt t at each point on trajector
pdf = new double[N]; // prob. density function at each point on trajectory.
113 pstat = new double[N]; // distribution which would relax to if driving were suddenly frozen
pstatpx = new double[N]; // eval at x+dx
115 pstatmx = new double[N]; // eval at x-dx
pstatpv = new double[N]; // eval at v+dx
117 pstatmv = new double[N]; // eval at v-dx
pstatep = new double[N]; //pstat evaluated at -v
119 str_pstatpx = new double[N]; // pstat evaluated at 0.5(x[j]+x[j+1])+dx
str_pstatmx = new double[N]; // at 0.5(x[j]+x[j+1])-dx
121 str_pstatpv = new double[N]; // at 0.5(v[j]+v[j+1])+dx
str_pstatmv = new double[N]; // at 0.5(v[j]+v[j+1])-dx
123 Straj = new double[N]; // cumulative total entropy production along trajectory
Ssysstraj = new double[N]; // cumulative system entropy
125 Smedtraj = new double[N]; // cumulative medium entropy
Straj1 = new double[N]; // cumulative S1
127 Straj2 = new double[N]; // cumulative S2
Straj3= new double[N]; // cumulative S3
129 dSsys = new double[N]; // incremental increase at timestep
dSmed = new double[N];
131 dS1 = new double[N];
dS2 = new double[N];
133 dS3 = new double[N];

135
// sample initial values from a boltzmann distribution at T0
137 x[0] = distribution(generator) * sqrt(boltzmannk*T0/kappa);
v[0] = distribution(generator) * sqrt(boltzmannk*T0/m);
139 temp[0] = T0*(1+A*(x[0]*x[0]/(2*boltzmannk*T0)));
//this is all which is required to calculate next x and v values.
141
// Initialize these to zero.
143 Straj[0]=0.0;
Ssysstraj[0]=0.0;
145 Smedtraj[0]=0.0;
Straj1[0]=0.0;
147 Straj2[0] = 0.0;
Straj3[0] = 0.0;
149 dSsys[0]=0.0;
dSmed[0]=0.0;
151 dS1[0]=0.0;
dS2[0] = 0.0;
153 dS3[0] = 0.0;

155 // begin main simulation of the kth trajectory
for(int j=0; j<(N-1); j++) {
157     x[j+1] = x[j] + v[j]*dt;
v[j+1] = v[j] - (gamma*v[j]*dt) - ((kappa*x[j])/m)*dt +
159     sqrt((2*boltzmannk*temp[j]*gamma)/m)*dW[j];
str_x[j+1] = 0.5*(x[j]+x[j+1]);
161 str_v[j+1] = 0.5*(v[j]+v[j+1]);

163 //define to simplify pstat expressions.
double skapT0 = A+B*sin(w*dt*j);
165 double skapT02 = A + B*sin(w*(j+1)*dt);

```

```

167 temp[j+1] = T0*(1+(A+(B*sin(w*(j+1)*dt)))*(x[j+1]*x[j+1]/(2*boltzmannk*T0)));
tempplus[j+1] = T0*(1+(A+(B*sin(w*(j+1)*dt)))*((x[j+1]+dx)*(x[j+1]+dx)/(2*boltzmannk*T0)));
169 tempminus[j+1] = T0*(1+(A+(B*sin(w*(j+1)*dt)))*((x[j+1]-dx)*(x[j+1]-dx)/(2*boltzmannk*T0)));
str_temp[j+1] = T0*(1+(A+(B*sin(w*j*dt)))*(str_x[j+1]*str_x[j+1]/(2*boltzmannk*T0)));
171 str_tempplus[j+1] = T0*(1+(A+(B*sin(w*j*dt)))*((str_x[j+1]+dx)*(str_x[j+1]+dx)
/ (2*boltzmannk*T0)));
173 str_tempminus[j+1] = T0*(1+(A+(B*sin(w*j*dt)))*((str_x[j+1]-dx)*(str_x[j+1]-dx)
/ (2*boltzmannk*T0)));
175
dtempx[j+1] = (A+B*sin(w*dt*(j+1)))*(x[j+1]/(boltzmannk));
177 dtempxplus[j+1] = (A+B*sin(w*dt*(j+1)))*((x[j+1]+dx)/(boltzmannk));
dtempxminus[j+1] = (A+B*sin(w*dt*(j+1)))*((x[j+1]-dx)/(boltzmannk));
179 str_dtempx[j+1] = (A+B*sin(w*dt*j))*(str_x[j+1]/(boltzmannk));
str_dtempxplus[j+1] = (A+B*sin(w*dt*j))*((str_x[j+1]+dx)/(boltzmannk));
181 str_dtempxminus[j+1] = (A+B*sin(w*dt*j))*((str_x[j+1]-dx)/(boltzmannk));

dtempt[j+1] = (x[j+1]*x[j+1]/(2*boltzmannk))*(w*B*cos(w*dt*(j+1)));

185 //Note constant factors left out as only concerned with log(pdf[j+1]/pdf[j]).
pdf[j+1] = sqrt((1/temp[j+1])*exp(-(m*v[j+1]*v[j+1]/(2*boltzmannk*temp[j+1]))
187 *pow((1+(A*x[j+1]*x[j+1]/(2*boltzmannk*T0)),-1*(kappa/A)-1))
*(1+(1/(4*gamma*temp[j+1]))*dtempt[j+1] + (1/(2*gamma*temp[j+1]))
189 *dtempx[j+1]*v[j+1] - (m/(4*boltzmannk*gamma*temp[j+1]*temp[j+1]))
*dtempt[j+1]*v[j+1]*v[j+1]-(m/(6*gamma*boltzmannk*temp[j+1]*temp[j+1]))
191 *dtempx[j+1]*v[j+1]*v[j+1]*v[j+1]));

193
pstat[j+1] = sqrt(skapT02/(2*M_PI*boltzmannk*T0))*(tgamma(1+(kappa/skapT02))/
195 tgamma(0.5+(kappa/skapT02)))*pow(temp[j+1],-1-(kappa/skapT02))
*sqrt(m/(2*M_PI*boltzmannk*temp[j+1]))*exp(-(m*v[j+1]*v[j+1])
197 / (2*boltzmannk*temp[j+1]))*(1+(1/(2*gamma*temp[j+1]))*v[j+1]*dtempx[j+1] -
(m/(6*gamma*boltzmannk*temp[j+1]*temp[j+1]))*v[j+1]*v[j+1]*v[j+1]*dtempx[j+1]);
199

201 pstatep[j+1] = sqrt(skapT02/(2*M_PI*boltzmannk*T0))*(tgamma(1+(kappa/skapT02))/
tgamma(0.5+(kappa/skapT02)))*pow(temp[j+1],-1-(kappa/skapT02))
203 *sqrt(m/(2*M_PI*boltzmannk*temp[j+1]))*exp(-(m*v[j+1]*v[j+1])
/ (2*boltzmannk*temp[j+1]))*(1-(1/(2*gamma*temp[j+1]))*v[j+1]*dtempx[j+1] +
205 (m/(6*gamma*boltzmannk*temp[j+1]*temp[j+1]))*v[j+1]*v[j+1]*v[j+1]*dtempx[j+1]);

207
str_pstatpv[j+1] = sqrt(skapT0/(2*M_PI*boltzmannk*T0))*(tgamma(1+(kappa/skapT0))/
209 tgamma(0.5+(kappa/skapT0)))*pow(str_temp[j+1],-1-(kappa/skapT0))
*sqrt(m/(2*M_PI*boltzmannk*str_temp[j+1]))*exp(-(m*(str_v[j+1]+dx)
211 *(str_v[j+1]+dx))/(2*boltzmannk*str_temp[j+1]))*(1+
(1/(2*gamma*str_temp[j+1]))*(str_v[j+1]+dx)*str_dtempx[j+1] -
213 (m/(6*gamma*boltzmannk*str_temp[j+1]*str_temp[j+1]))*(str_v[j+1]+dx)*
(str_v[j+1]+dx)*(str_v[j+1]+dx)*str_dtempx[j+1]);
215

217 pstatpv[j+1] = sqrt(skapT02/(2*M_PI*boltzmannk*T0))*(tgamma(1+(kappa/skapT02))/
tgamma(0.5+(kappa/skapT02)))*pow(temp[j+1],-1-(kappa/skapT02))
219 *sqrt(m/(2*M_PI*boltzmannk*temp[j+1]))*exp(-(m*((-1*v[j+1]+dx)
*((-1*v[j+1]+dx))/(2*boltzmannk*temp[j+1]))*(1+(1/(2*gamma*temp[j+1]))
221 *((-1*v[j+1]+dx)*dtempx[j+1]- (m/(6*gamma*boltzmannk*temp[j+1]*temp[j+1]))
*((-1*v[j+1]+dx))*((-1*v[j+1]+dx))*((-1*v[j+1]+dx)*dtempx[j+1]));
223

225 str_pstatmv[j+1] = sqrt(skapT0/(2*M_PI*boltzmannk*T0))*(tgamma(1+(kappa/skapT0))/
tgamma(0.5+(kappa/skapT0)))*pow(str_temp[j+1],-1-(kappa/skapT0))
227 *sqrt(m/(2*M_PI*boltzmannk*str_temp[j+1]))*exp(-(m*(str_v[j+1]-dx)
*(str_v[j+1]-dx))/(2*boltzmannk*str_temp[j+1]))*(1+
229 (1/(2*gamma*str_temp[j+1]))*(str_v[j+1]-dx)*str_dtempx[j+1] -
(m/(6*gamma*boltzmannk*str_temp[j+1]*str_temp[j+1]))*(str_v[j+1]-dx)
231 *(str_v[j+1]-dx)*(str_v[j+1]-dx)*str_dtempx[j+1]);

```

```

233 pstatmv [ j + 1 ] = sqrt ( skapT02 / ( 2 * M_PI * boltzmannk * T0 ) ) * ( tgamma ( 1 + ( kappa / skapT02 ) ) /
235 tgamma ( 0.5 + ( kappa / skapT02 ) ) ) * pow ( temp [ j + 1 ], - 1 - ( kappa / skapT02 ) ) *
sqrt ( m / ( 2 * M_PI * boltzmannk * temp [ j + 1 ] ) ) * exp ( - ( m * ( ( - 1 * v [ j + 1 ] ) - dx ) *
237 ( ( - 1 * v [ j + 1 ] ) - dx ) ) / ( 2 * boltzmannk * temp [ j + 1 ] ) ) * ( 1 + ( 1 / ( 2 * gamma * temp [ j + 1 ] ) )
* ( ( - 1 * v [ j + 1 ] ) - dx ) * dtempv [ j + 1 ] - ( m / ( 6 * gamma * boltzmannk * temp [ j + 1 ] * temp [ j + 1 ] ) )
239 * ( ( - 1 * v [ j + 1 ] ) - dx ) * ( ( - 1 * v [ j + 1 ] ) - dx ) * ( ( - 1 * v [ j + 1 ] ) - dx ) * dtempv [ j + 1 ] );

241
243 str_pstatpx [ j + 1 ] = sqrt ( skapT0 / ( 2 * M_PI * boltzmannk * T0 ) ) * ( tgamma ( 1 + ( kappa / skapT0 ) ) /
tgamma ( 0.5 + ( kappa / skapT0 ) ) ) * pow ( str_tempplus [ j + 1 ], - 1 - ( kappa / skapT0 ) )
245 * sqrt ( m / ( 2 * M_PI * boltzmannk * str_tempplus [ j + 1 ] ) ) * exp ( - ( m * str_v [ j + 1 ] * str_v [ j + 1 ] )
/ ( 2 * boltzmannk * str_tempplus [ j + 1 ] ) ) * ( 1 + ( 1 / ( 2 * gamma * str_tempplus [ j + 1 ] ) )
247 * str_v [ j + 1 ] * str_dtempvplus [ j + 1 ] - ( m / ( 6 * gamma * boltzmannk * str_tempplus [ j + 1 ]
* str_tempplus [ j + 1 ] ) ) * str_v [ j + 1 ] * str_v [ j + 1 ] * str_v [ j + 1 ] * str_dtempvplus [ j + 1 ] );

249
251 pstatpx [ j + 1 ] = sqrt ( skapT02 / ( 2 * M_PI * boltzmannk * T0 ) ) * ( tgamma ( 1 + ( kappa / skapT02 ) ) /
tgamma ( 0.5 + ( kappa / skapT02 ) ) ) * pow ( tempplus [ j + 1 ], - 1 - ( kappa / skapT02 ) )
253 * sqrt ( m / ( 2 * M_PI * boltzmannk * tempplus [ j + 1 ] ) ) * exp ( - ( m * v [ j + 1 ] * v [ j + 1 ] ) /
( 2 * boltzmannk * tempplus [ j + 1 ] ) ) * ( 1 - ( 1 / ( 2 * gamma * tempplus [ j + 1 ] ) ) * v [ j + 1 ]
255 * dtempvplus [ j + 1 ] + ( m / ( 6 * gamma * boltzmannk * tempplus [ j + 1 ] * tempplus [ j + 1 ] ) )
* v [ j + 1 ] * v [ j + 1 ] * v [ j + 1 ] * dtempvplus [ j + 1 ] );

257
259 str_pstatmx [ j + 1 ] = sqrt ( skapT0 / ( 2 * M_PI * boltzmannk * T0 ) ) * ( tgamma ( 1 + ( kappa / skapT0 ) ) /
tgamma ( 0.5 + ( kappa / skapT0 ) ) ) * pow ( str_tempminus [ j + 1 ], - 1 - ( kappa / skapT0 ) )
261 * sqrt ( m / ( 2 * M_PI * boltzmannk * str_tempminus [ j + 1 ] ) ) * exp ( - ( m * str_v [ j + 1 ] *
str_v [ j + 1 ] ) / ( 2 * boltzmannk * str_tempminus [ j + 1 ] ) ) * ( 1 + ( 1 / ( 2 * gamma *
263 str_tempminus [ j + 1 ] ) ) * str_v [ j + 1 ] * str_dtempvminus [ j + 1 ] -
( m / ( 6 * gamma * boltzmannk * str_tempminus [ j + 1 ] * str_tempminus [ j + 1 ] ) )
265 * str_v [ j + 1 ] * str_v [ j + 1 ] * str_v [ j + 1 ] * str_dtempvminus [ j + 1 ] );

267
269 pstatmx [ j + 1 ] = sqrt ( skapT02 / ( 2 * M_PI * boltzmannk * T0 ) ) * ( tgamma ( 1 + ( kappa / skapT02 ) ) /
tgamma ( 0.5 + ( kappa / skapT02 ) ) ) * pow ( tempminus [ j + 1 ], - 1 - ( kappa / skapT02 ) )
271 * sqrt ( m / ( 2 * M_PI * boltzmannk * tempminus [ j + 1 ] ) ) * exp ( - ( m * v [ j + 1 ] * v [ j + 1 ] ) /
( 2 * boltzmannk * tempminus [ j + 1 ] ) ) * ( 1 - ( 1 / ( 2 * gamma * tempminus [ j + 1 ] ) ) * v [ j + 1 ] *
273 dtempvminus [ j + 1 ] + ( m / ( 6 * gamma * boltzmannk * tempminus [ j + 1 ] * tempminus [ j + 1 ] ) )
* v [ j + 1 ] * v [ j + 1 ] * v [ j + 1 ] * dtempvminus [ j + 1 ] );

275 /* do not calculate an increment when j=0. Saves having to define the zero value of every
array being used separately, and negligible difference.*/
277 if ( j == 0 ) {
dSsys [ j + 1 ] = 0;
279 dSmed [ j + 1 ] = 0;
dS1 [ j + 1 ] = 0;
281 dS2 [ j + 1 ] = 0;
dS3 [ j + 1 ] = 0;
283 } else {
dSsys [ j + 1 ] = - ( log ( pdf [ j + 1 ] ) - log ( pdf [ j ] ) );
285
dSmed [ j + 1 ] = ( - 1 / ( boltzmannk * temp [ j ] ) ) * ( m / 2 ) * ( v [ j + 1 ] * v [ j + 1 ] - v [ j ] * v [ j ] ) -
287 ( kappa * x [ j ] / ( boltzmannk * temp [ j ] ) ) * v [ j ] * dt;

dS1 [ j + 1 ] = ( ( log ( str_pstatpx [ j + 1 ] ) - log ( str_pstatmx [ j + 1 ] ) ) / ( 2 * dx ) ) * ( x [ j + 1 ] - x [ j ] ) +
289 ( ( log ( str_pstatpv [ j + 1 ] ) - log ( str_pstatmv [ j + 1 ] ) ) / ( 2 * dx ) ) * ( v [ j + 1 ] - v [ j ] );
291
dS2 [ j + 1 ] = - ( v [ j ] * x [ j ] * dt / ( boltzmannk * temp [ j ] ) ) -
293 ( m * v [ j ] * ( v [ j + 1 ] - v [ j ] ) ) / ( boltzmannk * temp [ j ] ) -
( x [ j + 1 ] - x [ j ] ) * ( ( log ( pstatpx [ j ] ) - log ( pstatmx [ j ] ) ) / ( 2 * dx ) ) -
295 ( v [ j + 1 ] - v [ j ] ) * ( ( log ( pstatpv [ j ] ) - log ( pstatmv [ j ] ) ) / ( 2 * dx ) )
+ ( boltzmannk * temp [ j ] * gamma * dt / m ) * pow ( ( ( log ( pstatpv [ j ] ) - log ( pstatmv [ j ] ) ) ) / ( 2 * dx ) )
, 2 )

```

```

297         +v[j]*dt*((log(pstatpx[j])-log(pstatmx[j]))/(2*dx)) -
299         dt*(gamma*v[j]-(x[j]/m))*((log(pstatpv[j])-log(pstatmv[j]))/(2*dx));
301
302     dS3[j+1] = log((pstat[j]/pstat[j+1])*(pstatep[j+1]/pstatep[j]));
303
304 }
305 //cumulative of each entropy component along trajectory.
306 Ssysstraj[j+1] = Ssysstraj[j]+dSsys[j+1];
307 Smedtraj[j+1] = Smedtraj[j]+dSmed[j+1];
308 Straj[j+1] = Straj[j]+ dSmed[j+1] + dSsys[j+1];
309 Straj1[j+1] = Straj1[j] + dS1[j+1] + dSsys[j+1];
310 Straj2[j+1] = Straj2[j] + dS2[j+1];
311 Straj3[j+1] = Straj3[j] + dS3[j+1];
312
313 /* add cumulative value at each timestep to the average values for that timestep.
314 Divide by total no. trajectories later when data is analyzed, as data comes from
315 multiple runs of this code on the Legion cluster anyway*/
316 av_traj[j+1] += Straj[j+1];
317 av_traj_sys[j+1] += Ssysstraj[j+1];
318 av_traj_med[j+1] += Smedtraj[j+1];
319 av_traj_ds1[j+1] += Straj1[j+1];
320 av_traj_ds2[j+1] += Straj2[j+1];
321 av_traj_ds3[j+1] += Straj3[j+1];
322
323 } //end of j loop (end of trajectory)
324
325 //save values of stot (from 2pi/8 -> 6pi/8 here)
326 STOT[i] = Straj[N-1] - Straj[N-13334];
327 SITOT[i] = Straj1[N-1] - Straj1[N-13334];
328 S2TOT[i] = Straj2[N-1] - Straj2[N-13334];
329 S3TOT[i] = Straj3[N-1] - Straj3[N-13334];
330
331 //clear variables for next trajectory. Does lead to problems if this step isn't taken.
332 delete [] tempinit;
333 delete [] xinit;
334 delete [] vinit;
335 delete [] Straj1;
336 delete [] Straj3;
337 delete [] dS3;
338 delete [] pstatep;
339 delete [] dS1;
340 delete [] str_tempplus;
341 delete [] str_tempminus;
342 delete [] str_dtempplus;
343 delete [] str_dtempminus;
344 delete [] pstat;
345 delete [] str_pstatpv;
346 delete [] str_pstatmv;
347 delete [] str_pstatpx;
348 delete [] str_pstatmx;
349 delete [] Straj;
350 delete [] Smedtraj;
351 delete [] Ssysstraj;
352 delete [] x;
353 delete [] v;
354 delete [] temp;
355 delete [] dtempt;
356 delete [] dtemp;
357 delete [] pdf;
358 delete [] dSsys;
359 delete [] dSmed;
360 delete [] str_x;
361 delete [] str_v;
362 delete [] str_dtemp;
363 delete [] tempplus;
364 delete [] tempminus;

```

```

363     delete [] dtempplus;
364     delete [] dtempminus;
365     delete [] str_temp;
366     delete [] dS2;
367     delete [] Straj2;
368     delete [] pstatpv;
369     delete [] pstatmv;
370     delete [] pstatpx;
371     delete [] pstatmx;

372 } //end of simulation

373
374 //output data
375 double randno=rand()%100000+999;
376 ostreamstream os1;
377 ostreamstream os2;
378 ostreamstream os3;
379 ostreamstream os4;
380 ostreamstream os5;
381 ostreamstream os6;
382 ostreamstream os7;
383 ostreamstream os8;
384 ostreamstream os9;
385 ostreamstream os10;
386 os1 << "stottraj" << randno << ".txt";
387 os2 << "ssystraj" << randno << ".txt";
388 os3 << "smedmedtraj" << randno << ".txt";
389 os4 << "s1traj" << randno << ".txt";
390 os5 << "s2traj" << randno << ".txt";
391 os6 << "s3traj" << randno << ".txt";
392 os7 << "stohist" << randno << ".txt";
393 os8 << "s1hist" << randno << ".txt";
394 os9 << "s2hist" << randno << ".txt";
395 os10 << "s3hist" << randno << ".txt";
396 string str1 = os1.str();
397 string str2 = os2.str();
398 string str3 = os3.str();
399 string str4 = os4.str();
400 string str5 = os5.str();
401 string str6 = os6.str();
402 string str7 = os7.str();
403 string str8 = os8.str();
404 string str9 = os9.str();
405 string str10 = os10.str();
406 ofstream outone(str1);
407 ofstream outtwo(str2);
408 ofstream outthree(str3);
409 ofstream outfour(str4);
410 ofstream outfive(str5);
411 ofstream outsix(str6);
412 ofstream outseven(str7);
413 ofstream outeight(str8);
414 ofstream outnine(str9);
415 ofstream outten(str10);
416 outone.precision(10);
417 outtwo.precision(10);
418 outthree.precision(10);
419 outfour.precision(10);
420 outfive.precision(10);
421 outsix.precision(10);
422 outseven.precision(10);
423 outeight.precision(10);
424 outnine.precision(10);
425 outten.precision(10);
426
427 for(int l=0; l < N; l++) {

```

```
429     outone << av_traj[1] << " ";
      outtwo << av_traj_sys[1] << " ";
431     outthree << av_traj_med[1] << " ";
      outfour << av_traj_ds1[1] << " ";
433     outfive << av_traj_ds2[1] << " ";
      outsix << av_traj_ds3[1] << " ";
435 }

437 for (int h=0; h<k; h++) {
      outseven << STOT[h] << " ";
439     outeight << SITOT[h] << " ";
      outnine << S2TOT[h] << " ";
441     outten << S3TOT[h] << " ";
      }
443
      return 0;
445 }
```

# Appendix B

## Bibliography

- [1] Ford, I. and Spinney, R. (2012), *Fluctuation Relations: A Pedagogical Overview*, Wiley
- [2] Gibbs, J.W. (1902), *Elementary Principles in Statistical Mechanics*, Yale University Press
- [3] Seifert, U. (2008), *Stochastic thermodynamics: principles and perspectives*, Eur. Phys. J. B, 64 (3-4), 423 - 431.
- [4] Seifert, U. (2012), *Stochastic thermodynamics, fluctuation theorems and molecular machines*, Rep. Prog. Phys. 75 126001
- [5] Lahiri, S. (2008) *Total entropy production fluctuation theorems in a nonequilibrium time-periodic steady state*, arXiv:0811.0795v2 [cond-mat.stat-mech]
- [6] Speck, T., Blickle, V., Bechinger, C. and Seifert, U. (2007) *Distribution of entropy production for a colloidal particle in a non-equilibrium steady state*, EPL 79 30002
- [7] Ford, I. (2013), *Statistical Physics, An Entropic Approach*, Wiley
- [8] Papoulis, A. (1984), *Probability, Random Variables, and Stochastic Processes, 2nd ed.*, New York: McGraw-Hill
- [9] Harris R. and Schutz G. (2007), *Fluctuation theorems for stochastic dynamics*, J. Stat. Mech. (2007) P07020
- [10] Risken, H. (1989) *The Fokker-Planck Equation*, Springer-Verlag, New York
- [11] Gardiner, C. (1983) *Handbook of Stochastic Methods*, Springer
- [12] Sekimoto, K. (2010) *Lecture Notes in Physics, vol. 799, Stochastic Energetics*, Springer
- [13] Ford, I. and Spinney, R. (2012) *Entropy production in full phase space for continuous stochastic dynamics*, Phys. Rev. E 85, 051113
- [14] Oono, Y. and Paniconi, M. (1998) *Steady State Thermodynamics*, Prog. Theor. Phys. Suppl.130,29
- [15] Evans, D. and Searles, D, (2002) *The fluctuation theorem*, Adv. Phys., 51, 1529–1585
- [16] Jarzynski, C. (1997) *Nonequilibrium equality for free energy differences.*, Phys. Rev. Lett., 78, 2690.
- [17] Crooks, G.E. (1999) *Entropy production fluctuation theorem and the nonequilibrium work relation for free energy differences.*, Phys. Rev. E, 60, 2721–2726.

- [18] Krantz, S. (1999) *Jensen's Inequality*. §9.1.3 in *Handbook of Complex Variables*, Boston, MA: Birkhäuser, p. 118
- [19] Martyushev, L. and Seleznev, V. (2005), *Maximum entropy production principle in physics, chemistry and biology*, <http://dx.doi.org/10.1016/j.physrep.2005.12.001>
- [20] Byron, F. and Fuller, R. (1992), *Mathematics of Classical and Quantum Physics*, Dover Books on Physics
- [21] Stolovitzky, G. (1998), *Non-isothermal inertial Brownian motion*, *Physics Letters A*, 241, 240-256